Volume 21
Number 34
14 September 2025
Pages 6651–6824

Soft Matter

rsc.li/soft-matter-journal

ISSN 1744-6848

ROYAL SOCIETY OF CHEMISTRY

REVIEW ARTICLE
Martin Reifarth
(Sub-)microscale patterning *via* microcontact printing (μCP): recent advances, applications and future perspectives

20 YEARS ANNIVERSARY

Soft Matter

REVIEW

View Article Online
View Journal | View Issue

Cite this: *Soft Matter*, 2025, **21**, 6658

(Sub-)microscale patterning *via* microcontact printing (μCP): recent advances, applications and future perspectives

Martin Reifarth [ab]

Microcontact printing (μCP) is a versatile and low-cost technique for surface patterning, allowing for the fabrication of intricate designs with relative ease. However, despite these clear advantages, the application of μCP has predominantly focused on smooth, uniform surfaces, while rough, capillary-active, or hydrogel surfaces have largely been neglected in existing literature. This article aims to review the latest advances in μCP, tracing the evolution of patterning techniques and highlighting recent applications across various fields. Our discussion will encompass both fundamental developments in technology and practical implementations that illustrate its potential. In the last section, we will address the question why non-smooth surfaces have gathered less interest and aim to propose strategies for overcoming the inherent challenges they pose. With this contribution, we will also provide a perspective by shifting our focus to the specific challenges posed by capillary-active surfaces. We will introduce the innovative concept of polymer brush-supported μCP (PolyBrushMiC), which could serve as a promising strategy to address these challenges. By incorporating polymer brushes, we can enhance the compatibility of μCP with rough surfaces, enabling more effective pattern transfer and improved stability of printed features.

Received 7th April 2025,
Accepted 24th June 2025

DOI: 10.1039/d5sm00355e

rsc.li/soft-matter-journal

Introduction

Several applications, ranging from microelectronics,[1,2] biosensing,[3–5] information storage,[6,7] to optoelectronics[8,9] and many others take advantage from microstructured surfaces. Common patterning techniques, such as photo-,[10] dip pen,[11] electron,[12,13] or ion beam lithography,[14,15] often rely on tedious experimental protocols and require specialized instrumentation. Microcontact printing (μCP), as a soft lithography technique, provides a straightforward, efficient, and cost-effective alternative soft lithography technique for patterning. μCP can be considered a miniaturized version of a stamping process that is familiar from everyday office life. During the process, an elastomeric stamp, mostly prepared from polydimethylsiloxane (PDMS),[16] is exposed to a functionalization agent – the ink. When the inked stamp is brought into physical contact with a substrate, the ink gets transferred thereto, which occurs exclusively at the areas, where the stamp and the substrate are in physical contact. The simplicity of this approach renders μCP also scalable,[17] which is in contrast to the aforementioned other patterning techniques. A major advantage of μCP is attributed to the characteristics of PDMS that is used as an elastomer stamp: being cured from liquid precursors, it can be casted on a (sub-) microscale surface relief to mould its surface characteristics.[16] Accordingly, a surface master that had been prepared tediously in a previous step can be replicated with the elastomer, which is used to transfer its pattern to a substrate during the μCP process.

The downstream applications of surface-structures substrates require specific characteristics of the printing patterns. At a first glance, this comprises the printing precision. Under optimal conditions, μCP can achieve a printing resolution that goes down even to the low nanometre regime.[18] Second, the functionality of the printed areas is significant. The printing resolution is dictated by the ink characteristics. As such, the affinity between the ink and the substrate as well as the rheological behaviour of the ink play a crucial role. A good printing resolution is undermined by ink smearing, which is the uncontrolled, diffusive spreading of the ink at the substrate. An appropriate functionality is achieved, when functional ink molecules or materials are employed.

In most literature examples, μCP is applied on smooth substrates. As a pioneer example, Kumar and Whitesides used thiols in their first publication in the early 1990s, which they printed with a structured stamp on a smooth gold surface.[19] In this study, the authors employed an ink that efficiently adsorbs at the at the substrate. Other, similar, approaches take

[a] *Institute of Chemistry, University of Potsdam, Karl-Liebknecht-Str. 24-25, D-14476 Potsdam, Germany. E-mail: martin.reifarth@uni-potsdam.de*
[b] *Fraunhofer Institute of Applied Polymer Research, Geiselbergstr. 69, D-14476 Potsdam, Germany*

advantage of a similar transfer chemistry.[20] With these ink-substrate parings, very high printing precisions can be achieved, which can be attributed to a high affinity of the ink to the substrate.

Other substrates, particularly surfaces that possess a high capillary-activity, have sparsely been employed as μCP substrates. This can be attributed to the tendency of ink smearing, which would result in a poor printing resolution. Due to an expected ink smearing, also, printing under wet conditions is challenging. Wet printing, however, is crucial to maintain the functionality, *e.g.* of bioactive molecules.[21]

In this article, we therefore review current research activities in microcontact printing, focussing thereby on achievements within the last 15 years. In the last section, we explain, why capillary-active or hydrophilic substrates have been neglected in literature. With that, we discuss polymer-brush supported μCP (PolyBrushMiC), with which ink smearing can be reduced or entirely circumvented, so that said substrate classes become accessible with μCP.

μCP strategies for patterning smooth surfaces

Conventional μCP – self-assembling monolayers (SAMs), polymers and particles as inks

μCP was pioneered by Kumar and Whitesides, who initially described the transfer of self-assembling monolayers (SAMs) on a gold (Au) surface.[19] Assembling at smooth interfaces, SAMs have long been employed for the functionalization of Au surfaces,[22] using thiol-terminal long chain-alkyls compounds for functionalization. As a result of the balance between the strong chemisorption energy of the headgroup-substrate interaction and weaker interchain van der Waals forces, these compounds bind efficiently to the gold substrates, eventually yielding ordered SAM structures.[23] These effective interactions are exploited to print Au surfaces with alkylthiol surfaces using μCP,[24,25] rendering these ink-substrate interaction a textbook example of a successful μCP process. SAMs can be introduced possessing different qualities of the monolayer, which depends on the inking an printing conditions (Fig. 1).[26]

The ease of fabrication renders this ink-substrate pair an ideal system to validate new concepts of μCP. As an example, a roll-to-roll μCP process, which enables large-scale patterning, was assessed using 1-octadecylthiol as an ink.[17]

In this literature example, the ink was transferred efficiently, allowing the fabrication of gratings with line-widths of 300, 400, and 600 nm at various locations on a 4-inch plastic substrate at a speed of 60 cm min^{-1}.[17] In another example, gold surfaces micropatterned with a thiol-based corrosion inhibitor have been examined with respect to their mechanical stability.[27] The authors concluded, that gold micropatterns possessed a greater stability compared to substrates, which were decorated entirely with the thiol.

Alkylthiols are effective agents used for surface passivation, yielding hydrophobic areas. By using ω-functional alkylthiols, patterns with a dedicated chemical functionality can be introduced to a gold surface. As an example, thiol-functional ionic liquids were attached, rendering a functionalized surface area hydrophilic. By combining both methods – using μCP to apply one species and backfilling with the other – patterns with defined wetting abilities can be created.[28,29] The resulting patterns can be used for the deposition of droplets, which may act as reaction spaces[28] or as gas sensors (Fig. 2).[29]

Indeed, also other monolayers can be printed on different substrates. These will not be the subject of the present review article, as they have been reviewed elsewhere.[20]

While monolayers of functional molecules are effective for patterning surfaces like gold, other surfaces such as silica or glass require other specific surface functionalization agents. Polymers provide a more universal approach, as they can functionalize surfaces more efficiently due to their ability to bind non-specifically. They adsorb at the contact area and exhibit limited diffusion to non-printed areas.[16] The simplest method to introduce chemically functional polymers is by using a pristine PDMS stamp for patterning. PDMS, made from silicone oil precursors, will be crosslinked during the process of its curing. However, the curing process is never fully complete, leaving unreacted PDMS precursor oils within the stamp. Typically, the PDMS hardening includes a thorough washing step, during which the unreacted oils are removed. Using a PDMS stamp for patterning, for which the washing step is

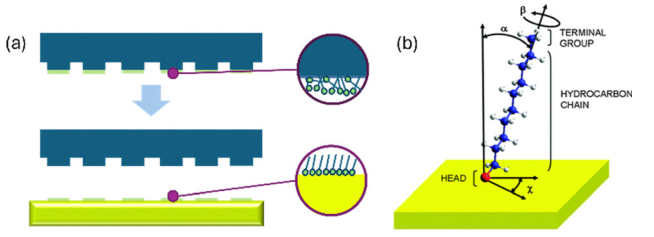

Fig. 1 Printing of a self-assembling monolayer (SAMs) using an alkylthiol on a gold surface. (a) Schematic overview over the printing process. (b) Binding of the alkylthiol to the surface. Reproduced with permission.[23] Copyright 2010, Royal Society of Chemistry.

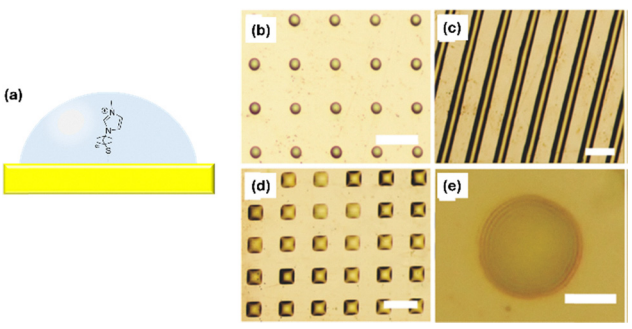

Fig. 2 Printing of ionic liquids for the deposition of microscale droplets. (a) Chemical structure of the ionic liquid printed on a gold surface. (b)–(e) Different printed patterns. The scale bars are (b) 50 μm, (c) 100 μm, (d) 50 μm, and (e) 10 μm. Reproduced with permission.[29] Copyright 2016, the American Chemical Society.

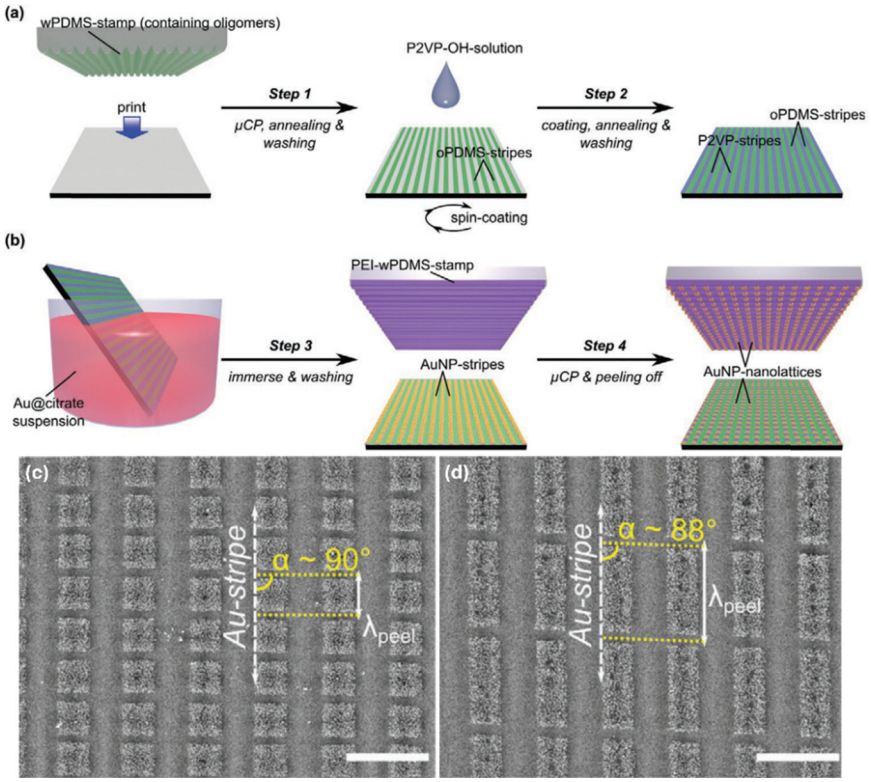

Fig. 3 Patterns of gold nanoparticles (AuNPs) introduced by printing with oligomeric PDMS (oPDMS). (a) Schematic representation of the printing. The introduced stripe pattern was subjected to backfilling with hydroxy-terminated poly(2-vinylpyridine) (P2VP-OH). (b) Immersing the patterned wafer in a gold nanoparticle suspension results in a selective deposition of the particles at the substrate. A subsequent peel-off process using a PDMS stamp with a positively decorated stamp yields gold nanoparticle lattices (c) and (d). Reproduced with permission.[31] Copyright 2020, Wiley.

intentionally skipped, allows for transferring oligomeric PDMS (oPDMS) to the substrate.[30,31] With the deposited patterns, other functionalization agents, such as polymers or colloids, can be guided to form respective patterns. As an example, Wang *et al.* printed stripe-patterns with oPDMS, which were backfilled with the positively charged poly(2-vinylpyridine) polymer to guide the adsorption of gold nanoparticles (AuNPs).[31] In a subsequent step, an additional stamp, fully surface-decorated with a cationic polyelectrolyte, was added to the substrate. Due to its positive surface charge, it could peel off gold particles, which resulted in the formation of AuNP lattices (Fig. 3).

More functional patterns can be transferred using polyelectrolytes.[32–35] As an example, the positively charged poly(ethylene imine) (PEI)[33–35] can be applied to pattern dissimilarly charged silica surfaces, where they adhere due to electrostatic interactions. Using polyelectrolytes with a particularly high molecular weight, the polymer shell can even be deposited as a thick layer.[34,35]

In a study by Kusaka *et al.*, the authors used a poly(*N*-vinylpyrrolidone) ink for the μCP fabrication of patterns exhibiting relatively thick films (~1.5 μm).[36] The authors used a Hertzian model to predict the efficiency of the ink transfer.

Polydopamine (PDA) is highly intriguing polymer accompanied by abundant favourable characteristics, such as a simple preparation process, good biocompatibility, strong adhesive properties and other,[37] rendering it useful for patterning different surfaces. Its adhesive properties, for instance, can be exploited to pattern glass or gold substrates.[38] In the respective examples, the polydopamine was prepared *in situ*, by oxidizing its monomeric unit dopamine on the PDMS stamp. Its adhesive properties can be used also for negative μCP.[39] In this case, a fluorinated substrate initially fully covered by polydopamine is addressed with a PDMS stamp. Due to the low surface energy, the PDA will stick to the stamp and thus lifted off from the substrate surface, leaving PDA surface patterns behind.

Analogously to polymers, nanoparticles can also be effectively used as ink for microcontact printing (μCP). For surface patterning, particles such as gold nanoparticles (AuNPs),[40–42] quantum dots,[43,44] or nanodiamonds[45] are applied for surface patterning. Efficient adsorption of these particles to the substrate can be achieved through electrostatic interactions[41,43] or by considering surface energy.[45]

Microcontact chemistry

In a traditional μCP process, small molecules, macromolecules or particles, which chemi- or physisorb onto the substrate, are used for patterning. Beyond, reactive molecules can be used as ink, which may react with specific features of the substrate surface. As a result, microcontact printing enables quick and precisely localized surface reactions, permitting molecular modification and patterning across various substrates. This approach facilitates reactive transfer even when working with

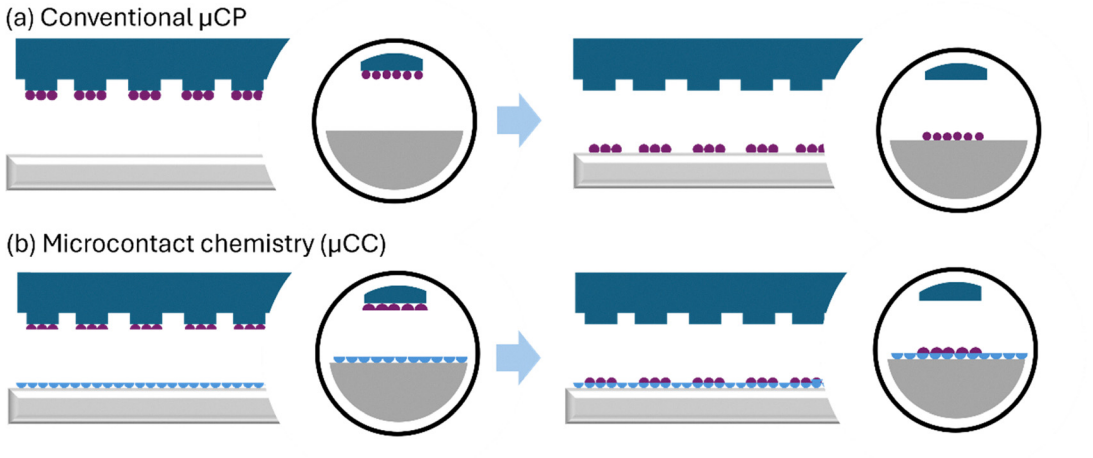

Fig. 4 Conventional microcontact printing (μCP) *vs.* microcontact chemistry (μCC). (a) In conventional μCP, the ink is transferred from the stamp to the substrate, where it physi- and chemisorbs. (b) In μCC, a reaction partner that is attached to the substrate is reacted with the ink, when the stamp and the substrate contact each other.

generally less reactive partners.[46,47] This process, referred to as the term "microcontact chemistry" (μCC) can be considered an advancement of the ordinary μCP process (Fig. 4).[46,48]

In a straightforward μCC approach, reactive inks are used to functionalise the substrate in a covalent fashion. In an illustrative literature example, Li *et al.*[49] demonstrated the utilization of (3-aminopropyl) triethoxysilane (APTES) to print on substrates like SiO_2, mica, quartz, sapphire, and glass coverslips. APTES, known for its capacity to covalently attach to oxidic surfaces, binds to the substrate and introduces an organo-bound amino functionality to the surface. Accordingly, the authors printed mono- or oligo-layers of APTES. They describe a rather simple approach, as they used a diluted APTES solution and inked a PDMS stamp by drop-casting. By adjusting the ink concentration, they could control the thickness of the layers. Diazoaryls, as highly reactive intermediates, react with gold or carbon surfaces, where they form covalent bonds under the release of molecular nitrogen (N_2). Consequently, diazo compounds can be used for μCP to directly pattern substrate surfaces.[50,51] For this purpose, the respective aromatic amino compounds are either directly diazotized using $NaNO_2$ in an acidic environment,[50] or they are electro-grafted[51] to pattern the substrate.

While in the aforementioned examples, reactive molecules were printed on a pristine SiO_2 or Au surface, in other examples, anchors are printed on a surface, which are used for the growth of functional inorganic materials. Accordingly, layers of inorganic compounds could be added to a substrate.[52,53] As an example, ruthenium oxide (RuO_x) layers were patterned.[52] This protocol starts from patterns of $RuCl_3$ on a substrate added *via* μCP, which function as an anchor for a subsequent atomic layer deposition (ALD) process. Using ruthenocene as a precursor, several cycles of ALD were conducted, which resulted in the growth of a RuO_x film that formed exclusively on the patterned areas. In another example, carboxylate patterns – which were introduced by μCP – were used as an anchor.[53] In a subsequent process, the growth of metal–organic frameworks (MOF) was initiated, using $Zn(NO_3)_2$ and terephthalic acid as MOF building blocks.

In early examples of μCC, chemical functionalities at the substrate are activated by a reaction partner offered by the stamp.[54,55] In detail, the stamps were functionalized with sulfonic acids, while *N-tert*-butyloxycarbonyl-(Boc-) protected amino functionalized substrates were used. During the direct contact, protons dissociating from the sulfonic acid participate in the deprotection reaction, which yields functional amino patterns.[54,55] In other examples, amino-functional inks were printed on activated carboxylate-surfaces:[56,57] accordingly, the reaction of amino functions with NHS-activated[56] or carboxylic acid fluorides were exploited.[57] Further strategies involve the deployment of aldehydes for μCC.[58,59] Accordingly, amino-terminal peptides were printed on aldehyde-terminal silica surface functions.[58] In a reductive amination process, the ink was covalently attached to the substrate. In another example, an aldehyde function was added to a protein, which was transferred to an oxime-terminal surface function.[59]

Sharpless and colleagues coined the term "click chemistry" to describe a concept involving highly modular and stereospecific reactions driven by a strong thermodynamic force, enabling the synthesis of complex substances from smaller units *via* heteroatoms.[60] This widely adopted principle is also applicable to μCC. A prominent such click-type reaction is the conversion of epoxides with amino functions. Due to their enhanced ring strain, epoxides undergo a ring-opening reaction under nucleophilic attack of the amine. This type of the reaction had been deployed for the functionalization of polymer microspheres,[61,62] which include glycidyl-functional monomers. Another click reaction type is Diels–Alder cycloaddition. In this case, a diene undergoes a thermally driven cycloaddition resulting in the formation to yield a six-membered ring. This reaction type has been used to pattern a Si wafer with carbohydrates possessing cyclopentadiene (Cp) anchors to a maleimide-functional surface.[63] Here, the Cp-functional sugar ink acts as the diene, while the substrate maleimide is the dienophile. In another example, a substrate offering a furane-functional polymer film is patterned.[64] In this case, the ink is functionalized with the highly efficient dienophile

maleimide. Due to the thermal reversibility of this process, the resulting patterns could also be erased simply by a thermal treatment of the sample.[64] The reaction of thiols and terminal alkenes or alkynes is another prominent click-type reaction. Accordingly, thiols react with the respective alkenes or alkynes to yield stable thioethers under UV irradiation. In a UV-assisted μCC process, both reaction types have been used for surface patterning.[65–67]

Table 1 Selected stamp/substrate pairs used for microcontact chemistry.te is reacted with the ink, when the stamp and the substrate contact each other

Reaction partners	Patterned substrate	Ref.
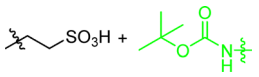		54,55
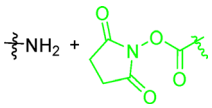	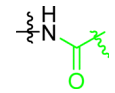	56
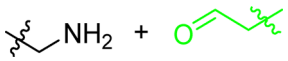	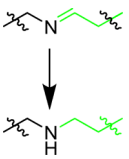	58
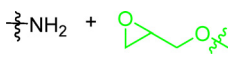	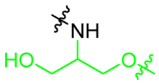	61,62
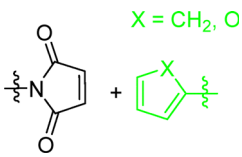	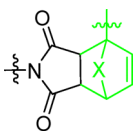	63,64
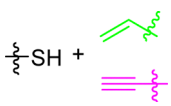	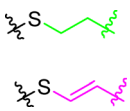	65–67
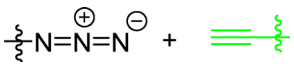	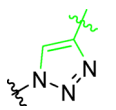	43,53,59,62,65,67,68
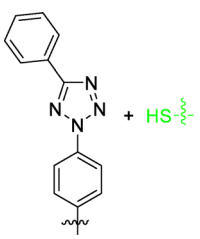	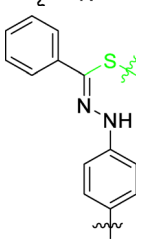	69
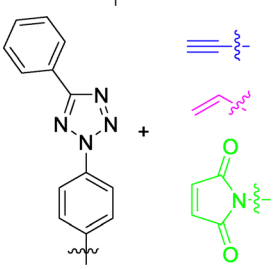	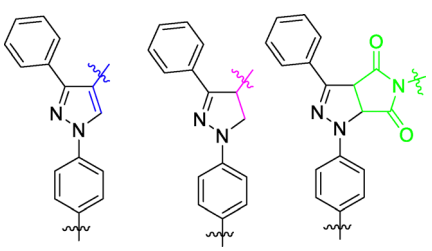	69
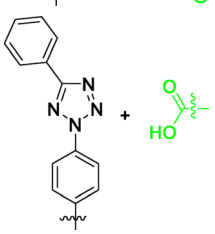	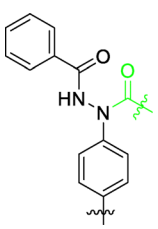	70

One of the most eminent click reactions is the Huisgen-type copper-catalyzed azide–alkyne click (CuAAC) reaction. During this process, a terminal alkyne and an azide undergo a 1,3-dipolar cycloaddition to yield a five-membered triazole ring. Due to its high efficiency, this reaction has also been applied in μCC.[43,59,62,65,67,68] Accordingly, this reaction was implemented in protein,[59] or particle[43] patterning or the fabrication of patchy microspheres among others.[62] Interestingly, the aforementioned different click approaches are orthogonal reactions, rendering them suitable for "multicolour printing",[62,67] where two or more consecutive printing processes using different ink materials are deployed.

Moreover, Ravoo and co-workers introduced tetrazoles as a reactive intermediate suitable for a click-type μCC.[69,70] These are five-membered heterocycles including one carbon and for nitrogen atoms, were introduced as a substrate decoration. Upon irradiation with UV light, they eliminate nitrogen to yield a reactive intermediate. Accordingly, they can react with maleimides, thiols, alkenes, alkynes[69] or even carboxylic acids,[70] to yield stable reaction products for surface decoration. An overview over different chemical principles deployed in microcontact chemistry is provided in Table 1.

Alongside click reactions, also other, rather complex chemistries have been established for surface patterning. Specifically, these were applied to add bioactive molecules to the surface. As an example, Wu *et al.* prepared protein surface patterns exploiting the specific interaction of nickel (Ni) ions and His-tagged proteins.[71] In detail, a surface decorated with nitrilotriacetic acid (NTA), a chelating agent, was first printed with nickel ions. In a second step, proteins modified with a His-tag were applied, which bound exclusively to the printed areas.[71] In another literature example, carbohydrates were used for patterning. Patterning with sugar molecules, such as mannose, can, *e.g.* be used for selective cell attachment.[68] In an approach published by Buhl *et al.*, the authors conducted an *O*-glycosylation with a benzyl protected mannose on a surface.[72] For this purpose, they added the acetylated mannose to a hydroxy-terminal substrate. Contacting this surface reaction mixture with trimethylsilyl triflate (TMSOTf) acting as a catalyst, they induced the glycosylation reaction at the substrate (Fig. 5).

Polymer brushes

While in previous examples, solutions of polymers were used as ink, which were transferred from the stamp to the printed area, other literature examples focus on the introduction of polymer brushes to the printed patterns.[48] The term polymer brush refers to polymer chains that are terminally tethered densely to a surface. Being present in a confined environment, polymer brushes are often strongly extended, leading to a rather thick polymer film, enabling the introduction of a high density of functional molecules into the brush matrix. Polymer brushes can be prepared through either a *grafting to*- or *grafting from*-approach (Fig. 6). While in the *grafting to*-approach, polymer chains are attached to the surface using their starting group as a suitable anchor, in a *grafting from*-approach, a functional molecule is first attached to the surface, which serves as the starting group for a subsequent living polymerization step.[73,74] Polymer brush-patterned surfaces are also discussed in-depth elsewhere.[48]

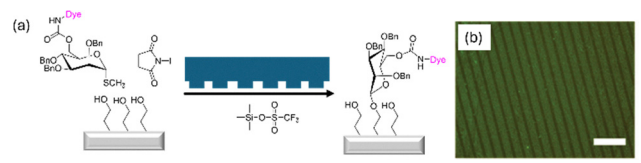

Fig. 5 μCC for binding a carbohydrate (mannose) *via* glycosylation to a hydroxy-functional surface. (a) Chemical principle. To the substrate, a stamp with the catalytically active species TMSOTf is added. (b) Pattern of mannose formed by μCC. The scale bar is 50 μm. Reprodcued with permission.[72] Copyright 2017, the Royal Society of Chemistry.

For microscale patterning of polymer brushes *via* a grafting to-approach, polymers synthesized by a reversible-addition–fragmentation chain-transfer (RAFT) polymerization were employed. In an example provided by Vonhören *et al.*, the authors started with a Si substrate that was patterned with a reactive silane offering a cycopentadiene moiety by means of micromolding in capillaries (MIMIC), a technique that is similar to μCP (Fig. 6).[75] Grafing was accomplished by offering different acrylate polymers, *i.e.* poly(acrylic acid), poly(2-hydroxyethyl acrylate) or poly(tetraethyleneglycol acrylate), which carry a trithiocarbonate function as a RAFT end group. Upon the exposure with the patterned substrate, the electron-deficient RAFT terminal group was underwent a Diels–Alder click reaction with cyclopentadiene moieties, which had been introduced as a pattern on a Si substrate using μCP in a previous step. Whereas *grafting to* constitutes a straightforward and versatile approach to add a pre-synthesized polymer to a surface, allowing for its in-depth characterization, this approach generally comes along with the drawback of a low grafting density.

In contrast, the *grafting from*-approach is often the preferred approach to introducing polymer brushes with a higher grafting density. This strategy requires the introduction of living radical polymerization starting groups to the substrate. As an example, α-bromisobutyric acid-derived molecules can be introduced as a monolayer on a substrate, facilitating a subsequent polymer grafting from a surface with the atom transfer-radical polymerization (ATRP) method (Fig. 6). Accordingly, ω-ATRP intitiator-functional alkylthiols were attached as SAMs to a gold surface using μCP with a PDMS stamp. Next, the ATRP initiators were used to graft polymer brushes, *e.g.* poly(*N*-isopropylacrylamid) (PNIPAAm) from the surface patterns.[76]

In another study, ATRP initiators were patterned *via* click chemistry to the substrates. A more in-depth discussion about the nature of this chemistry is provided in Section 2.2 of this article. Accordingly, substrates functionalized with terminal alkenes were subjected to a μCP process using 1,2,4,5-tetrazines as an ink. As electron-deficient dienes, 1,2,4,5-tetrazines undergo an inverse electron-demand Diels–Alder click reaction.[77] The patterned substrates were used for grafting of poly(methyl acrylate) brushes from the surface. Whereas

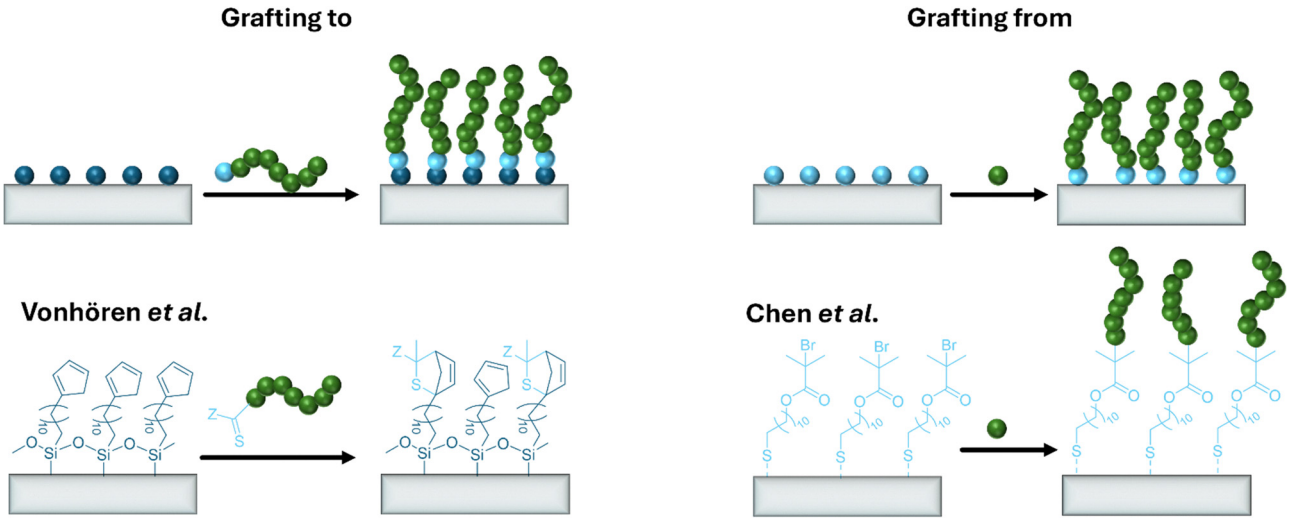

Fig. 6 Grafting to *vs.* grafting from-approach. The approach from Vonhören *et al.* is illustrative for the grafting to,[75] by Chen *et al.* for the grafting from-approach.[76]

1,2,4,5-tetrazine printing requires approximately one hour of printing duration,[77] in another study, the authors optimized this method by employing a triazolene dione-bound ATRP initiator as an ink to bind on an indole-functionalized substrates.[78] Triazolenes react with dienes and alkenes in Diels–Alder and Alder–ene reactions rather rapidly.[79] The method was utilized to graft poly(methyl acrylate) brushes from the surface.[78] In a *trans*-click reaction with an appropriate reaction partner at elevated temperature, the indole substrate could be regenerated, facilitating an erasure of the brush patterns previously introduced.[78]

As an application, polymer brush stripe patterns were introduced to convey adhesive characteristics to two different plates made of glass and substrate. In these examples polymer brushes are advantageous, since they offer a high number of chemical functionalities with a high spatial density. Stripe patterns of said polymer brushes are beneficial, since they enhance the roughness of the substrate, enabling the different brush patterns to interlock.[80,81] In an initial study, the authors fabricate brush patterns possessing a phenylboronic acid function, while its counterpart offers catechol moieties. In contact, both brush types show strongly adherent properties, which can be weakened by the addition of carbohydrates, which bind to boronic acids as well, competing with the catechols.[81] In a subsequent study, the authors utilize supramolecular interactions for this purpose, deploying aryl azapyrazoles and cyclodextrines as partners.[80]

In addition to these examples, where simple brush patterns are prepared, more intricate surface patterns have been described in literature. In this context, multiple μCP processes can be deployed, in the sense of a "multicolour μCP". As an example, Buhl *et al.* started with a substrate, to which a nitroxide-mediated polymerization (NMP) initiator has been attached, facilitating the introduction of a polymer brush consisting of 1,1,1,3,3,3-hexafluoroisopropyl acrylate and 7-octenylvinyl ether as reactive monomers.[82] Being selectively addressable for sequential post-modification with thiols and amines, the substrate has been subjected to multicolour μCP.[82]

In another study, Zauscher and co-workers demonstrate dynamic μCP, encompassing a dynamic ("moving") or a static ("jumping") relocation of the stamp on the substrate during μCP to introduce ATRP initiators on a gold surface (Fig. 7).[83] Analysis of the subsequently fabricated polymer brushed revealed intricate surface patterns of smeared or merged dots.

Alongside gold surfaces, being addressable with functional thiol linkers, or Si or glass substrates, which become accessible after the functionalization with a suitable silane surface modification agent, also other substrates have been patterned with initiators for a subsequent surface grafting. As an example, Kettling *et al.* used photochatalytically active TiO_2 surfaces, which they patterned with hydroxy-terminal alkylsilanes.[84] Photochemical activation rendered the surface redox-active, facilitating the selective oxidation of 2-aminoethanol. As a result, brushes of linear poly(ethylene imine) of ~50 nm resulted as an oxidation product of 2-aminoethanol. In a different approach, an amino-functional pyrene (Pyr-CH_2-NH_2) is used to pattern an oxidic silicon substrate.[85] Due to its amino-functionality, it adheres to the substrate *via* hydrogen bonding. As a result of a strong π-stacking capability, the pyrene adds as an oligomeric surface layer to the previously formed pyrene monolayer at the substrate. Showing strong adherence to the substrate, on the one hand, but on the other hand also offering amino functionalities for amide coupling, an ATRP initiator can be covalently attached to the surface, facilitating polystyrene grafting to the surface patterns.[85]

With a controlled growth of polymer brushes from a patterned 2D surface, the substrate surface morphology is extended to the third dimension. This was demonstrated by Wei *et al.*, who used a substrate that was entirely functionalized with brushes of different polymers, such as poly(2-hydroxyethyl methacrylate) (PHEMA), poly(*N*,*N*′-dimethylaminoethyl methacrylate) (PDMAEMA), poly(methyl methacrylate) (PMMA) or polystyrene (PS).[86] The authors wanted to stratify the brush substrate with a patterned second layer of polymer brushes. For this purpose, they patterned the brush matrix with

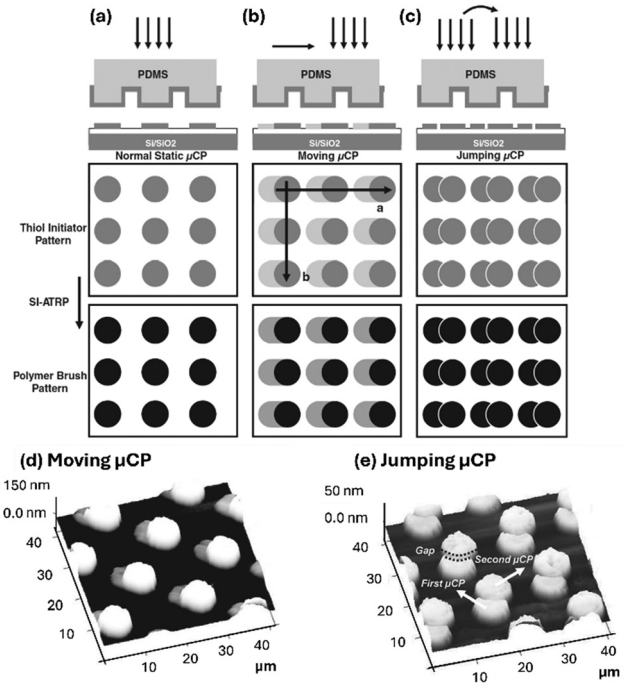

Fig. 7 Dynamic μCP. (a) In contrast to static μCP, dynamic moving (b) or jumping (c) μCP yields intricate patterns. Grafting polymer brushed from the printing areas yields polymer brush patterns as shown in (d) (for moving μCP) and (e) (for jumping μCP), respectively. Reproduced with permission.[83] Copyright 2011, Wiley.

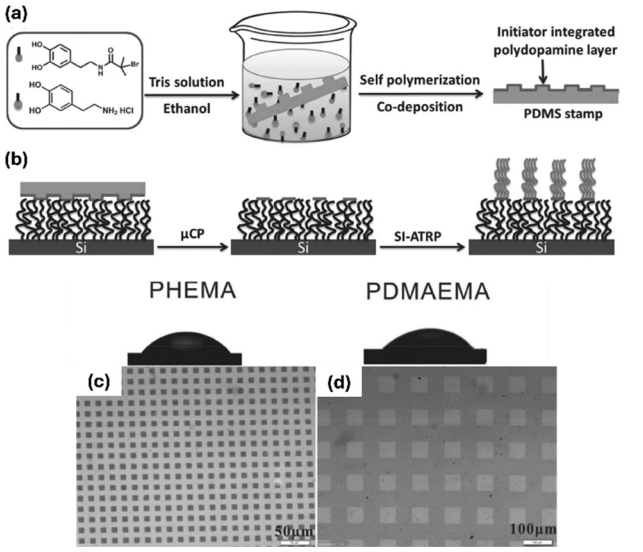

Fig. 8 Fabrication of stratified polymer brushes. (a) Dopamine, along with an ATRP initiator-functionalized dopamine derivative, were oxidized to form a polydopamine layer at a PDMS stamp. The polydopamine layer was (b) printed to a polymer brush matrix. With the ATRP initiator, a surface-initiated ATRP (SI-ATRP) was conducted, yielding polymer brushes of poly(2-hydroxyethylmethacrylate) (PHEMA) (c) and poly(2-*N*,*N*′-dimethylaminoethylmethacrylate) (PDMAEMA) (d). (c) and (d) Optical images. Reproduced with permission.[86] Copyright 2014, Wiley.

polydopamine, to which dopamine modified with an ATRP initiator was co-polymerized (Fig. 8).[86] With the addition of ATRP initiators, a second polymer brush layer could be grafted from the initial substrate.

Grafting polymer with cross-linkable units can allow a hardening of the polymer matrix subsequently to the grafting process. This was demonstrated by Lienkamp and colleagues, who prepared polymers containing a low percentage of different UV cross-linkable repeat units, *i.e.* nitrobenzoxadiazole (NBD), coumarin (COU), and/or benzophenone (BP), as comonomers.[87] UV crosslinking resulted in the preparation of gel-like structures, which could be tuned in their height (3 to 750 nm), depending on the crosslinker composition.

Applications of μCP

μCP of bioactive molecules: using proteins as ink

Alongside small molecular weight compounds, polymers or colloidal particles, bioactive macromolecules, such as proteins, can be used as inks for μCP. Protein patterning adds biological functions to the patterned surfaces, paving the way to application fields such as cell cultivation, sensing, the fabrication of devices, as reviewed elsewhere.[88]

As an example, enzymes have been employed as μCP inks in surface patterning. In one study, glucose oxidase (GOx) and lactase (Lac) were patterned on a functional gold surface.[89] The thiol sidechains of proteins were added to an alkene-functional surface and immobilized *via* the thiol–ene click reaction, maintaining their functionality post-immobilization. Similarly, the enzyme silicateine was directly patterned on a gold surface by exploiting the chemisorption of the thiol-functional enzyme to the gold support.[90] This enzyme's polycondensation activity was used to grow a photo-catalytically active TiO_2 layer on the surface. While this study focused on enzyme-based surface layer construction, Ganesh *et al.* showcased the destructive potential of an enzyme.[91] They printed a lipase, extracted from *Candida albica*, on a poly(ε-caprolactone) (PCL) film, where the enzyme's hydrolysis activity selectively digested the PCL film.

Alongside these examples, which demonstrated enzyme patterning, a main application field for μCP in the context of surface patterning with proteins is the utilization of the printed patterns as cell culture platforms.[88] Usually, in a tissue surrounding, cell behaviour is regulated by the extracellular matrix (ECM),[92] a complex 3D microenvironment that surrounds and embeds cells, which offers topographical and chemical cues that significantly influence cellular fate.[93] Inspired by the functions that ECM exhibit, scientists have used microcontact printing (μCP) to engineer surface properties that mimic these functions, creating precise patterns that influence cell behaviour.[94] This technique has been particularly effective in studying contact guidance, where cells align with anisotropic cues, affecting their cytoskeleton and subsequent behaviour.[88] Illustrative studies demonstrated that the growth of adherent cells is significantly affected by the surface features the cells attach to. When cells were cultivated on solid substrates exhibiting patterns of the protein fibronectin, their alignment and shape will be influenced by these patterns (Fig. 9).[95,96]

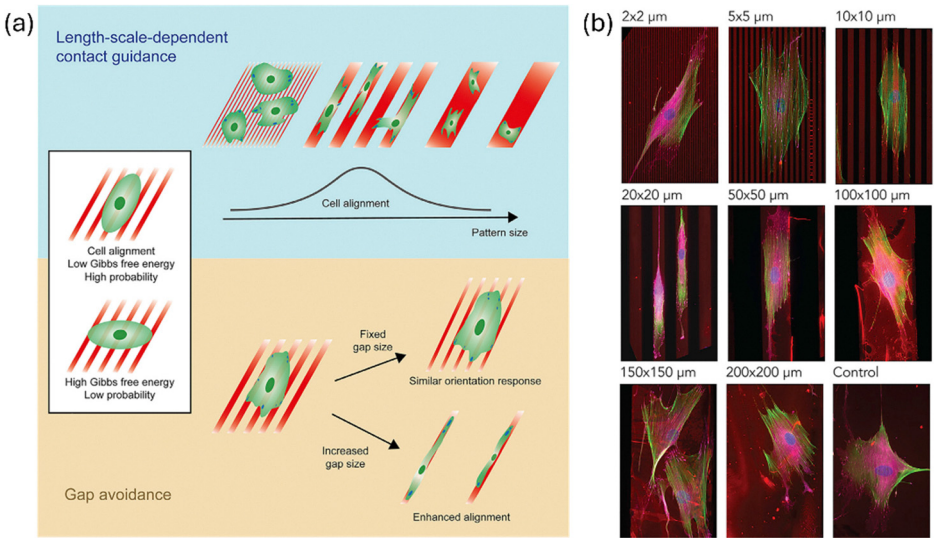

Fig. 9 Influence of printed fibronectin patterns on the alignment of myofibroblast cells. (a) Schemativ representation. (b) Micrographs of different pattern sizes (stripe width × space) influencing cell growth. In the micrographs, the fibronectin is labelled red, the focal adhesions are magenta, the actin cytoskeleton is green, and the nuclei are blue. Reproduced with permission.[96] Copyright 2020, Elsevier.

Being capable of fostering the selective growth of cells at the substrate, µCP protein patterns have been used to culture functional models of tissue-like structures.

As an example, the growth of nerve cells has been investigated,[21,97–100] using for instance beta-amyloids,[97,98] collagen[100] or laminin and poly(L-lysine)[101] as protein patterns. Fricke *et al.* found, that the growth of axons could be guided by discontinuous gradient patterns of laminin.[101] Endothelial cells like HUVCs were guided to form vascular patterns, which were guided by a fibronectin pattern introduced by µCP.[102] As a template, the authors used an ordinary plant leaf, whose veins mimic branching vasculature.

These examples underscore the potential of protein patterns for cell cultivation. However, it is crucial to consider how the proteins will be bound to the surface. For protein patterning on silica or glass surfaces, the respective surfaces are often pretreated with an alkoxysilane, which is used for the reactive immobilization of the protein.[4,95,103] In a similar fashion, polystyrene substrates were functionalized by plasma ion immersion implantation, which added functions to the surface that enabled covalent protein immobilization.[104] Alongside substrate modification, also stamp modification can be implemented to improve the µCP transfer. As an example, Jang *et al.* added a thin agarose layer to the stamp surface, which repelled the protein ink layer during the stamping process.[105] This procedure facilitated wet conditions during the printing process, which is favourable in order to ensure protein functionality.[21] In a rather interesting approach by Borowiec *et al.*,[106] protein transfer *via* µCP was combined with polymer embossing. An inked stamp was applied to a polycarbonate foil, and during the thermoforming process, the stamp's morphology was imprinted onto the foil while simultaneously transferring the protein layer to the foil (Fig. 10).

Covalent attachment of patterned proteins allows for precise control over their orientation on the surface. As an example, Lam and colleagues studied the effect of fibronectin orientation on vascular smooth muscle cell behaviour.[95]

They functionalized fibronectin with maleimide and reacted it with a mercapto-functionalized surface pattern. They compared two scenarios: one, where fibronectin was printed directly onto the surface, resulting in its random orientation, and another where an immobilization anchor was printed first, followed by directional protein binding. The study found that the binding mode significantly influenced cell growth.

Alternative immobilization strategies involve binding *via* streptavidin,[107] activated *N*-hydroxysuccinimide (NHS) active ester,[108] or benzylguanine, which is susceptible to the nucleophilic attack of a SNAP-tag functional protein.[109]

Alongside the actual protein functionalization, the surface features of the non-printed support will affect cell behaviour as well. Poly(ethylene glycol) (PEG), being a highly hydrophilic and

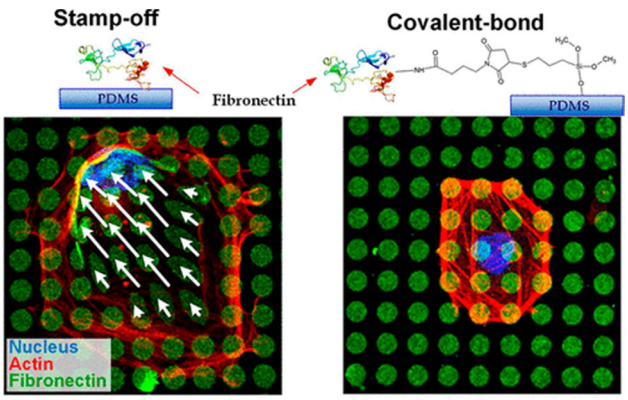

Fig. 10 Printing of fibronectin with a dedicated orientation. In the respective study,[95] fibronectin patterns printed with random orientation *vs.* patterns with a directed orientation are used for cell cultivation. Reproduced with permission.[95] Copyright 2018, the American Chemical Society.

non-ionic polymer, serves as an excellent antifouling coating.[110] Consequently, PEG-decorated surfaces typically repel cells. This makes it advantageous to print cell-guiding proteins onto PEG hydrogel coatings: while cells will adhere to the areas functionalized with the ECM protein, they will be repelled at the non-printed PEG areas, ensuring they remain only in the printed regions.[108,111,112] For surface functionalization of PEG hydrogel coatings, different strategies can be employed. The polymer matrix can be coated with polydopamine,[112] which serves as an anchor for further functionalization, or end group-functional PEG coatings can be used, providing an anchor group for direct protein functionalization.[108]

Poly(*N*-isopropylacryl amide) (PNIPAAm) is a thermoresponsive polymer with a lower critical solution temperature (LCST). Below this temperature, the polymer is hydrophilic, while it becomes hydrophobic at higher temperatures. As a result, confluent cells adhere to the support when PNIPAAm is hydrophobic and can be detached when the support is cooled, making PNIPAAm-coated cultivation dishes switchable active surfaces. In an illustrative study, the authors use a PNIPAAm-coated cultivation dish at a temperature > LCST, to which they print patterns of fibrinogen.[113] The patterned dishes were used for the selective growth of human dermal fibroblast (NHDF) cells. Afterward, the interspaces were backfilled with bovine artery endothelial cells, resulting in the formation of a bicellular 2D tissue model. Lowering the temperature below the LCST caused the cells to detach while remaining intact as a cell association. In a similar fashion, other thermally expendable hydrogels were addressed by μCP.[114,115] Specifically, polyethers were used for this purpose, which were addressed by first printing a layer of polydopamine, which was used for protein deposition in a second step.[114] In another study, gels like gelatine could be printed directly with the protein, when the gels were present in a freeze-dried state.[115] The transfer of a protein from the stamp to a hydrophilic substrate demands a deeper understanding of the underlying processes.

In order to understand the transfer of a polymer from a stamp to a hydrogel mechanistically, Ricoult *et al.* studied the influence of the surface energies of both the stamp and the substrate under humidified conditions.[116]

Building on these concepts, there are some further intriguing applications of cell manipulations using microcontact printing (μCP) on hydrogels. In one example, the ability to print switchable substrates was used to create anisotropic, "patchy" cells (Fig. 11).[117] A polyelectrolyte "ink" was printed on a PNIPAAm surface, and the pattern was used for cell seeding. After some time, the temperature was lowered below the LCST, releasing the cells while the ink remained at the cell interfaces, providing anisotropic functionalization. The study demonstrated the self-assembly behaviour of these cells using the patches as active sites (Fig. 11).[117]

In a further study, fibronectin islands were printed on a polystyrene substrate.[118] The islands were backfilled with pluronic, which acted as a repellent coating. These patterns were used to manipulate viable sperm cells, with the pattern serving as a trap for a single sperm, facilitating the analysis of individual cells. Pan and co-workers addressed the intricacy to print on soft and tacky samples. Accordingly, they printed patterns of ECM proteins in a first instance on a poly(vinyl alcohol) (PVA) layer in a first step.[119] The layer, when dried, forms a free-standing film, which can be transferred to the area of interest. In a second step, the film gets hydrated. During this step, the polymer film dissolved, leaving the protein surface patterns behind.

Preparation of anisotropic colloidal particles

Utilizing a flexible stamp for surface patterning enables the elastomeric PDMS to conform to the substrate renders μCP an effective technique for functionalizing curved interfaces. When considering colloidal particles as substrates with a curved surface, μCP can be used to introduce anisotropic functionalization in the contact area (Fig. 12).[48] The resulting patchy particles are

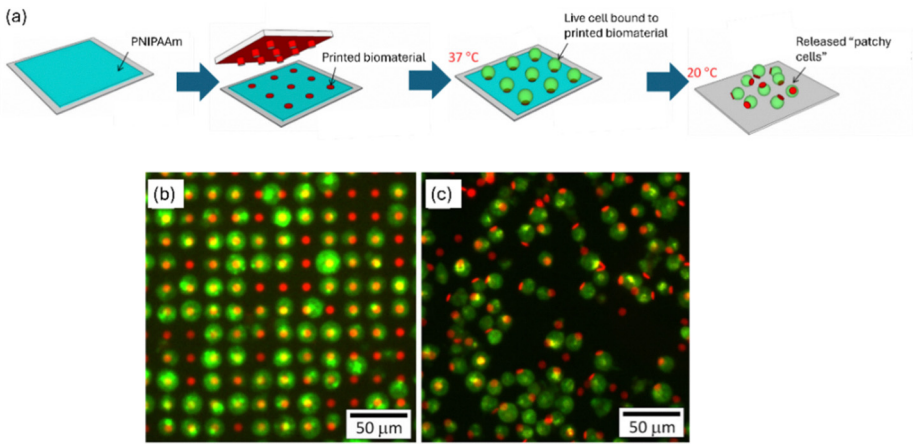

Fig. 11 Fabrication of patchy cells. (a) Schematic representation of the process. A polyelectrolyte is printed on a PNIPAAm surface using μCP. On this surface, cells are seeded. The cells can be released at a temperature of 20 °C. (b) K562 cells (green fluorescence) immobilized on the printed μCP array of a circular polyelectrolyte multilayer (red fluorescence) before being released. (c) Fluorescence micrograph of the cell–microparticle complexes after the release at 20 °C. Reproduced with permission.[117] Copyright 2015, Elsevier.

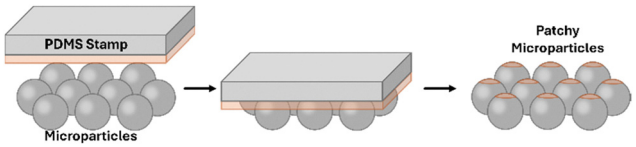

Fig. 12 Fabrication of patchy particles using a monolayer of microparticles.

characterized by possessing distinct surfaces domains, which differ either in morphology, or in chemistry (or both) from the residual surface of the particle.[120] With this functionalization, the particles inherit a surface asymmetry, rendering them highly interesting materials that show a directed, self-propulsive motion[121] or that can be deployed for self-assembly processes to facilitate the bottom-up synthesis of intricate complex systems.[122,123] Among other methods, μCP is a very valuable tool to fabricate patchy particles, which is capable to add very functional materials to the particles.[48]

To add functional areas to a particle, Zimmermann *et al.* utilized a monolayer of SiO_2 microspheres and added poly(ethylene imine) (PEI) as an ink to the particle cap.[33] Specifically, the group exploited the electrostatic attractions between the silica particles exhibiting a negative surface charge and PEI, which possesses an overall positive charge in an aqueousenvironment. In a follow-up publication, the authors could show that, depending on the removal of the particles from the stamp subsequently to the printing process, the particles obtained either a patch representing a thick layer of the polyelectrolyte at the particle (which the authors refer to as "3D patches"), or a very thin layer ("2D patches").[34] After the printing process, the particles adhered to the stamp surface. In order to release the particles, they were sonicated in a solvent environment. By careful selection of the solvent, the authors were able to control the morphology of the patch areas (Fig. 13). In detail, they used acetone to produce 3D, and ethanol for 2D patches. By transferring PEI from a wrinkled PDMS stamp, the authors could transfer stripe-like patterns, constituting a negative imprint of the wrinkle surface, to the particle cap.[35] Due to the accessibility of amino functions, PEI can be subjected to chemical functionalization, allowing, *e.g.* the introduction of biotin and avidin to the particle patches, which in turn can be used for self-assembly.[34] Naderi Mehr *et al.* printed different polyelectrolytes to melamine formaldehyde (MF) microspheres (~5 μm).[124] MF, which is tuneable in surface charge depending on external pH conditions, could, thus, be patched with positively charged PEI, and on the other hand also addressed with the polyanionic poly(methylvinylether-*alt*-maleic acid) (PMVEMA). The authors could identify different pH regimes, where the particle body (MF) and the patch are either similarly or oppositely charged, resulting in attractive or repulsive interactions.[124,125]

Beyond the introduction of a single patch by printing a functionality to a monolayer of particles, also a second patch can be introduced, using a method referred to as sandwich printing μCP.[33,124] For this purpose, the particle monolayer, adhering to the stamp after the first printing process, is addressed with a second stamp from the opposite particle side. With that method, Naderi Mehr *et al.* could add both polymer species to the same particle.[124] More intricate microscale anisotropic materials were fabricated in a layer-by-layer approach using polyelectrolytes.[126] Specifically, the authors of the respective study deposited a polymer multilayer, consisting of poly(allylamine hydrochloride) (PAH) and poly(diallyldimethyl ammonium chloride) (PDAC) as a cationic and poly(styrene sulfonate) (PSS) as anionic polyelectrolytes, by a layer-by-layer approach. The multilayer was next deposited on a substrate that in turn was coated with poly(vinyl alcohol) (PVA) by a μCP process (Fig. 14). Immersing the substrate in water resulted in PVA dissolution, releasing the printed layer-by-layer structures, which kept relatively stable in water. The polyelectrolyte surface remained stable, facilitating the addition of a further polymer layer. With that method, the authors succeeded to print finer structures on the microscale objects by applying a second μCP process onto the previously prepared microstructures.[126] In the previous examples, polyelectrolyte inks were employed to functionalize microscale particulate materials. These polymeric

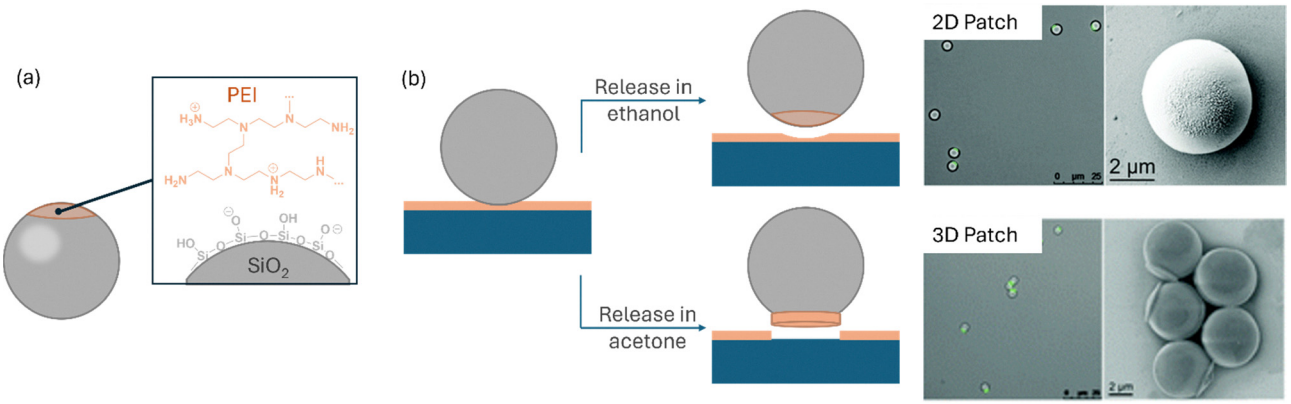

Fig. 13 Fabrication of patchy particles using poly(ethylene imine) (PEI) ink. (a) Schematic representation of the process. (b) Depending on the solvent, the particles either obtain a two-dimensional or a three-dimensional patch, depending on the solvent used for the particle release. The printed particles are observed with widefield fluorescence microscopy and scanning electron microscopy. The image in (b) is reproduced with permission.[34] Copyright 2018, the Royal Society of Chemistry.

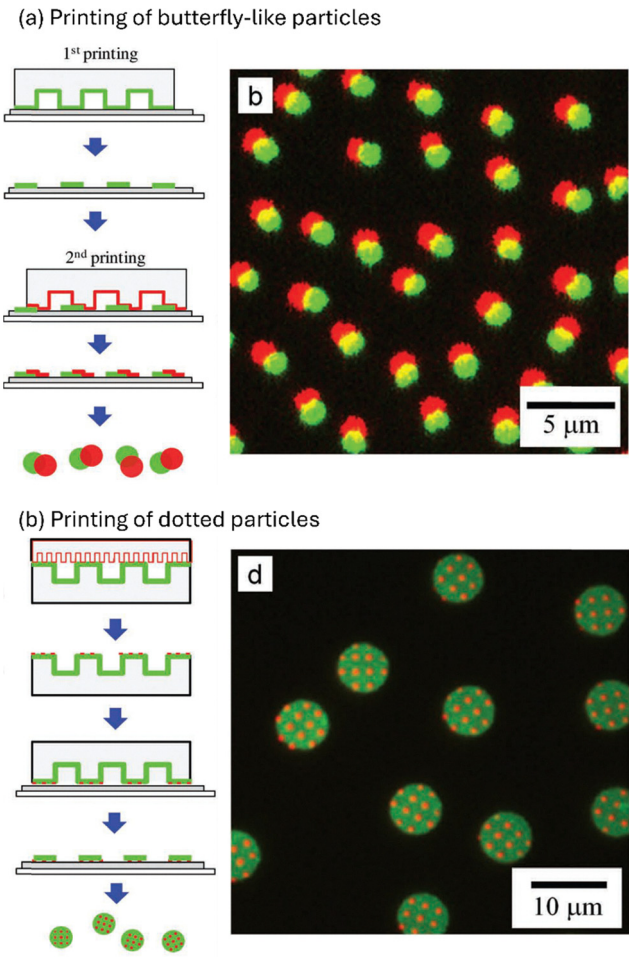

Fig. 14 Printing of anisotropic microparticles created by a layer-by-layer approach. (a) Printing of butterfly-like particles. (b) Printing of dotted particles. Reproduced with permission.[126] Copyright 2011, Wiley.

substances adhere to the particles solely through electrostatic interactions, eliminating the need for chemical treatments to attach the ink to the particle cap, which in turn simplifies the fabrication of these patchy particles. However, electrostatic interactions are susceptible to external factors, such as changes in pH levels or ion strength of the surrounding medium, which can affect the stability of the patches. It seems, therefore, advantageous to develop a strategy that enables the covalent attachment of functional molecules to particles. The method of microcontact chemistry (μCC) addresses this issue (further discussion is provided in section "Microcontact chemistry").

There are different μCC protocols described which are used for the fabrication of patchy particles. Accordingly, particles must possess a chemical function, which is complementary to a function that the ink material is supposed to possess, so that both can react in a click reaction. As an example, amino-functional dyes have been added to particles possessing epoxy functionalities (Fig. 15).[61,62,127] The particles, which were fabricated in a microfluidic setup using glycidyl methacrylate as a comonomer, could be transferred to bipatchy sandwich-type particles. Using amino-functional particles, an isothiocyanate-containing fluorescent label could be added as an ink.[128] In other publications, alkyne inks were printed on azide- or thiol-functional particles, exemplifying the feasibility to use copper-catalysed azide–alkyne or thiol–yne click chemistry,[62] complemented by a study using alkene-functional particles to add a thiol-ink using the thiol–ene click reaction.[129] With these methods, particles with a sandwich-type bipatchy architecture can be fabricated, which even may comprise bifunctional characteristics. The method is also capable of functionalizing particles in the low micrometre range (<6 μm).[62]

However, in these examples, merely fluorescent labels are incorporated inks.

While fluorescent dyes lack functionality, Sagebiel *et al.* demonstrated, that more functional materials can be added as particle patches (Fig. 16).[130] Specifically, the authors employed a triazolene dione-bound ATRP initiator as an ink, which was printed to vinyl functionalised silica particles *via* μCC, enabling a rather rapid functionalization reaction. With the introduced

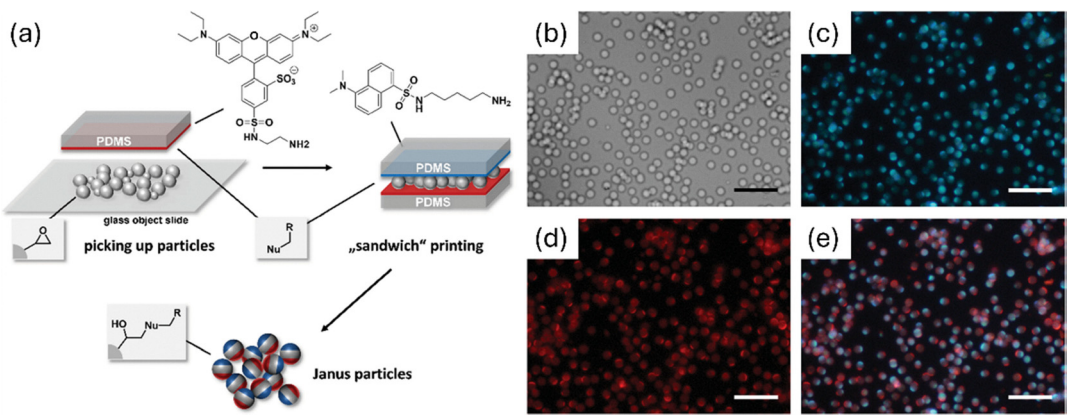

Fig. 15 Preparation of sandwich-type particles. (a) Overall scheme of the process to print amino-functional fluorescent dyes on microscale particles. (b) Transmission light micrographs. Fluorescence micrographs of (c) dansyl and (d) sulforhodamine fluorescent signals. (e) Overlay of both fluorescent signals. Scale bars are 20 μm. Reproduced with permission.[61] Copyright 2016, Wiley.

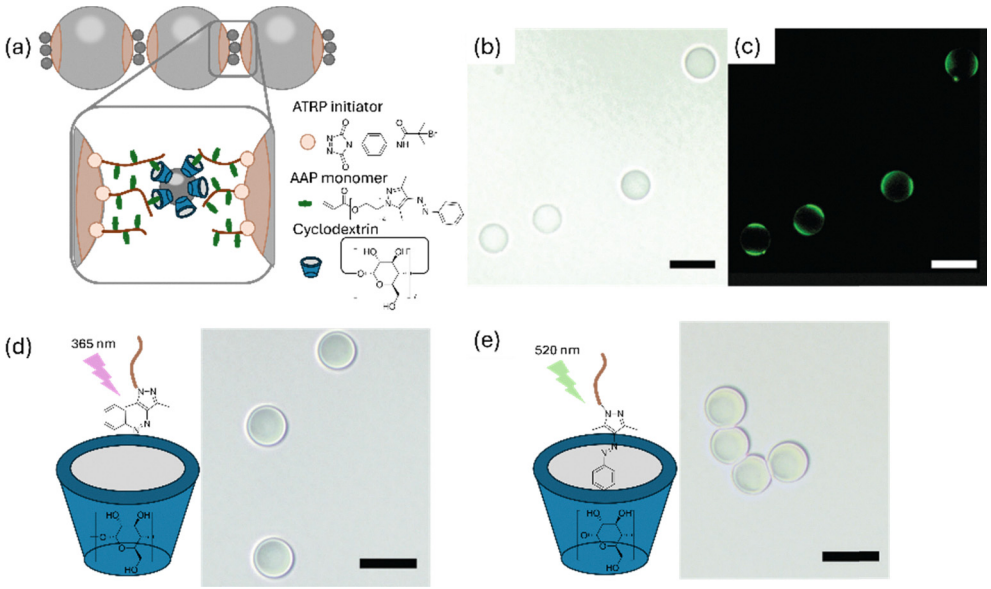

Fig. 16 Self-assembly of sandwich-printed SiO_2 microspheres. (a) Schematic representation of the particle. The SiO_2 microspheres (light grey) are assembled using functionalized iron oxide nanoparticles (dark grey). The SiO_2 patches are polymer materials consisting of a reactive ATRP initiator and an AAP monomer. The iron oxide nanoparticles are functionalized with cyclodextrine. (b) Transmission microscopy and (c) fluorescent microscopy images of the sandwich-printed microspheres. (d) Transmission microscopy image of microspheres with nanoparticles, where the AAP molecules have been switched to the (Z) state (showing no interaction with the nanospheres) by UV irradiation, and (e), where the AAP molecules have been switched to the (E) state (showing interaction with cyclodextrin and thus self-assembly) by irradiation with 520 nm. The scale bars are 10 μm. Reproduced with permission.[130] Copyright 2017, the Royal Society of Chemistry.

initiator, the authors were able to graft functional polymer from the surface. Containing arylazopyrazole (AAP) functionalities, the brushes could be used in self-assembly processes. For this purpose, iron oxide nanoparticles, which are surface-functionalized with β-cyclodextrine (CD), were added to the sandwich particles. The iron oxide nanoparticles, adhering to the brushes *via* AAP-CD supramolecular host–guest interactions, were used as a colloidal adhesive for the microspheres to form particle chains.[130] This supramolecular interaction, however, merely occurs, when the AAP is switched to its (*E*)-isomer (which in turn is triggered by irradiation with green light of 520 nm wavelength). When the AAP is in its (Z)-state when illuminating with UV light (365 nm), the interaction does not occur. Accordingly, the particles assemble after light activation, while they may be dis-assembled by illumination with UV light.

Using a polymer-brush assisted μCC protocol for the functionalization of inorganic oxide surfaces,[131] we were able to print primary alkyl amines to the surface of a silica particle (a further discussion on that topic will follow in the section "Microcontact printing unlimited"). The amino function was used to anchor a xanthate moiety to the particle, which can be utilized as a chain-transfer agent in a RAFT process.[132,133] With this method, we were able to graft different acrylic acid-derived polymers from the particle surface.[131]

While the aforementioned protocols favour the fabrication of mono- or sandwich-type bipatchy particles, also other patch geometries are accessible. Using a polymer brush-supported μCP process,[131] which will be outlined in more detail in the last section of this article, we were able to add up to four patches to silica microspheres that are positioned at the equatorial site of the particle, possessing a C_{2v} symmetry. The fabrication of such particles can be achieved, when they experience a spatial confinement of a channel of the PDMS stamp, whose dimensions match the particle diameter (Fig. 17).[134]

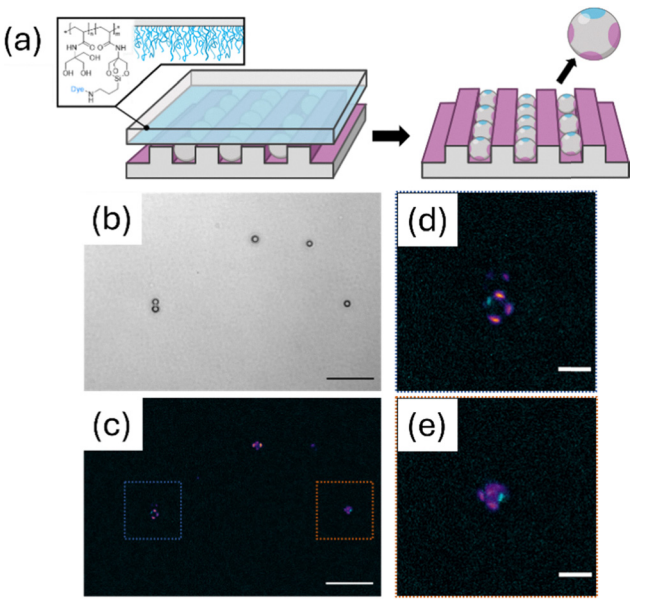

Fig. 17 Patchy particles fabricated in a confined environment. (a) Schematic representation. (b) Transmission light microscopy image of the particles. (c) Fluorescence microscopy image. (d) and (e) Zoom-in views of the particles. Scale bars: (b) and (c) 25 μm. (d) and (e) 5 μm. Reproduced with permission.[134] Copyright 2025, Wiley.

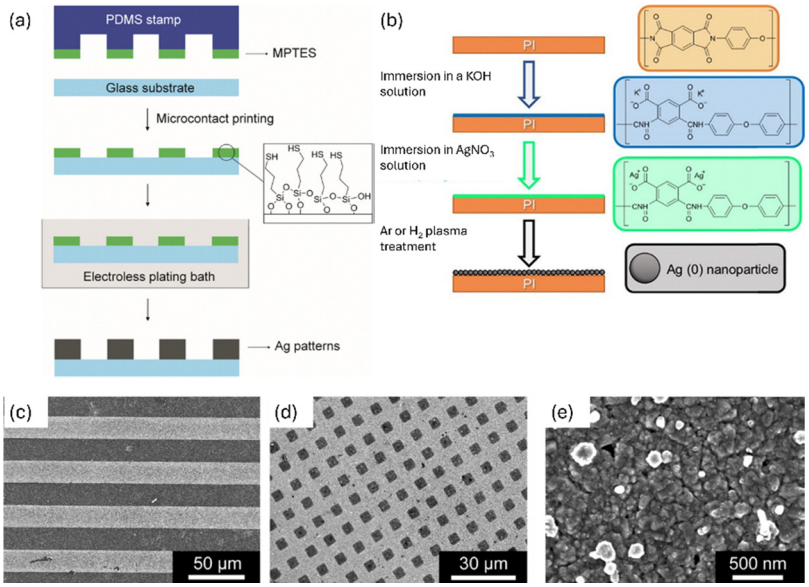

Fig. 18 Printing of AgNPs by using a silver precursor. (a) Schematic representation of the process using a MPTES,[142] and (b) a polyimide polymer.[143] (c) and (d) Printed particle patterns and (e) zoom-in thereof.[142] Reproduced with permission.[142,143] Copyright 2013 and 2014, Elsevier.

Printing of conductive inks for electronic applications

The patterning of micro- and nanostructured conductive patterns on insulating substrates is essential for advancements in microelectronics. In this context, microcontact printing (μCP) is a cost-effective method suitable for large-area applications, making it an ideal technique for fabricating microscale devices such as thin-film transistors.[135–137] Beyond, its compatibility with soft and flexible materials to be used as a substrate renders it suitable for the fabrication of flexible electronic devices that can be used in smart clothing and other applications.[138,139] The fabrication of conductive patterns with soft lithography demands conductive materials used as an ink for μCP.

These comprise metal nanoparticles, liquid metal alloys, conductive polymers and others.

Silver nanoparticles (AgNPs) serve as a prime example of a conductive ink. Using AgNPs directly as an ink, μCP was utilized to pattern various surfaces,[137,140,141] facilitating the fabrication of a thin-film resistor[140] or to print customized patterns on a flexible plastic foil.[141] Other studies start from silver ion (Ag^+) precursors, which are used for patterning, and which are chemically reduced to silver nanoparticles in a subsequent step.[142,143] As an example, substrates were mercapto-functionalized to coordinate silver ions, which were reduced to silver in a subsequent process (Fig. 18a and c–e).[142] In another study, the authors used a polyimide polymer for silver ion immobilization, yielding a rather uniform pattern of AgNPs (Fig. 18b).[143]

Conversely, Yoon *et al.* applied a selective etching technique, starting from a substrate entirely functionalized with silver nano-objects and masking of a pattern with μCP, allowing for selective etching of the non-masked part of the substrate.[144] Specifically, the authors used silver nanowires, which were selectively masked by μCP of uncured PDMS precursors. After curing, the PDMS remained as a barrier, protecting the underlying wires during an etching process. In addition to silver nanoparticles, also other metal nanoparticles were used for microscale patterning. As an example, Miller *et al.* used copper nanoparticles for surface functionalization.[145] In detail, the authors patterned an aluminium porphyrin complex to a substrate, which was used as an anchor for a catalyst, which in turn was used for promoting the electroless deposition of copper particles (Fig. 19).[145]

In a different study, metal precursors, *i.e.* Pt and Pd salts, were printed at different substrates, such as glass and polymer

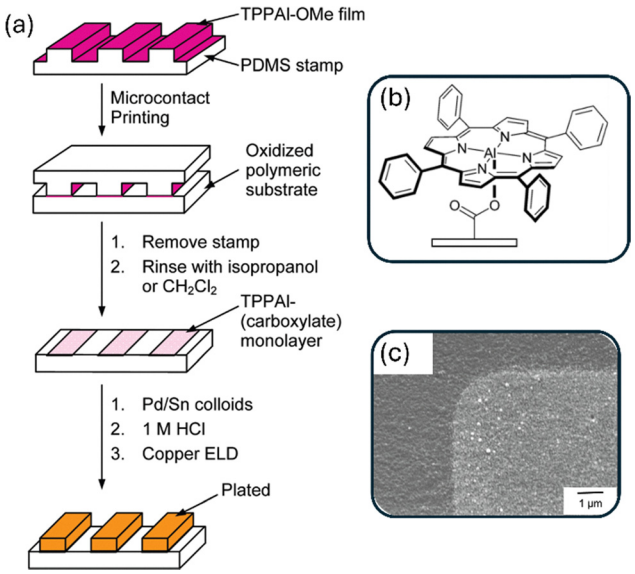

Fig. 19 μCP of a copper nanoparticle array using an aluminum porphyrin as an anchor. (a) Overall scheme. (b) Binding of the porphyrin complex serving as an anchor for copper nanoparticle formation. (c) Scanning electron micrograph of the printed pattern. Reproduced with permission.[145] Copyright 2010, the American Chemical Society.

films, using poly(ethylene glycol) (PEG) as a macromolecular carrier agent of the salts.[146] These patterns could be chemically reduced forming thick films (~30 nm thickness) of the respective Pt and Pd metals, showing a rather low electrical resistance of 1.1 to 6.7 Ω m. This example points toward the fact that metal film electronics promise a good conductivity, however, at the expense of an enhanced flexibility of the printing patterns. In order to overcome this issue, other studies report the use liquid metal alloys as an ink.[138,139,147]

Specifically, an eutectic gallium–indium (EGaIn) ink is deposited in to the microchannels of an elastomeric stamp. From there, the ink may be transported to flexible substrates. The resulting printing patterns exhibit a good conductivity even after mechanical stress.[147]

Carbon nanomaterials offer a low-cost, sustainable platform to be used as an ink for μCP. Graphene oxide (GO) is a two-dimensional, conducting material, that can be used directly as an ink for μCP.[148] As these materials adhere to hydroxyl-functional SiO_2 substrate, they can be utilized for patterning to fabricate conductive surfaces. Other literature examples employ carbon nanotubes (CNTs) as conductive materials.[135,149–152] In different studies, their transfer from the stamp to the substrate was investigated.

Béduer *et al.* identified ethanol an ideal solvent, which promotes CNT transfer,[150] while Mehlich *et al.* used the CNTs' affinity to dendrimers (Fig. 20),[135] and Ogihara *et al.* embedded the CNTs in a polymer matrix to ensure its transfer.[151] The resulting patterns are flexible, highly conductive and relatively untoxic, which renders them suitable sensing patters, that can *e.g.* be exploited to monitor the electric activity of neuronal cells.[152] In addition to carbon nanomaterials, also conductive polymers can be utilized as an ink. In a study from Garcia-Cruz *et al.*, the authors first selectively bind pyrrole to a surface.[153]

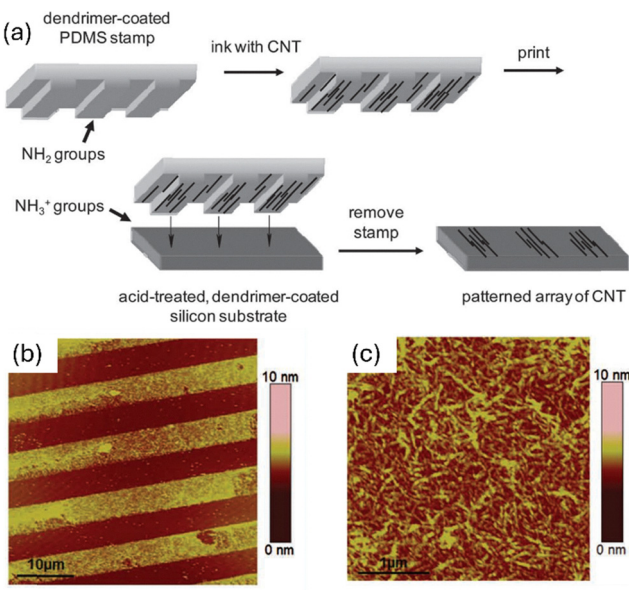

Fig. 20 Printing of carbon nanotubes (CNTs). (a) Schematic overview. (b) Printing pattern. (c) Zoom-in view of the printed pattern. Reproduced with permission.[135] Copyright 2012, Wiley.

The surface pattern was utilized to initiate a graft polymerization, resulting in the formation of polypyrrole films. These films were characterized as conductive films.

Microcontact printing unlimited: towards a polymer brush-supported μCP (PolyBrushMiC) routine to overcome ink smearing

μCP is a simple, straightforward, and cost-effective technique which is compatible with large-area patterning. Nevertheless, the majority of applications described earlier primarily involve smooth substrates patterned through microcontact printing (μCP), such as glass, mica, polished silicon, metals, or plastic foils, as it is discussed in the previous sections of this review article. In contrast, micro-rough substrates have received less attention, despite their relevance in coating applications[154] and their potential uses, *e.g.* in catalysis,[155] stem cell cultivation,[156] and other areas. This also applies to hydrogel surfaces promising applications in cell cultivation,[157] which should ideally be patterned under fully hydrated and buffered conditions *e.g.* to maintain the functionality of bio-active proteins.[21] Why have these surfaces largely been neglected as μCP substrates?

In order to achieve an efficient printing process, two critical parameters must be considered: (i) a high printing precision and (ii) a dedicated functionality of the ink, so that small patterns are created that possess defined chemical characteristics. Even though polymer materials, nanoparticles or proteins can be efficiently utilized as μCP inks (as outlined in the previous sections of this review article), defined chemical functionalities will be introduced using low molecular weight-compounds as inks (low molecular weight-inks – LMWI). Achieving a high precision with LMWI, however, is demanding due to ink mobility on the substrate, leading to uncontrolled ink smearing. In particular, when aiming to extend the method to a lower scale, specifically targeting nanometer-level printing precision – which we refer to as nanocontact printing (nCP) – the issue of ink smearing poses a particular challenge. Nevertheless, ink smearing can be mitigated if the ink has a high affinity for the substrate, such as reactive molecules that assemble as monolayers.

As already outlined, another important factor to obtain a high printing precision that is often overlooked is the substrate's characteristics: for accurate printing, the substrate should be not possess capillary-active characteristics (Fig. 21a), since severe ink smearing counteracts high printing precision (Fig. 21b). In addition, if a hydrogel substrate is supposed to be patterned, it should not be present in a hydrated state for accurate patterning, as the ink may dissolve in the solvent rather than being distributed on the substrate surface.

We must, therefore, consider how to control the ink diffusion on the stamp surface during the μCP process, allowing merely the transfer to the substrate without diffusive distribution on the substrate surface or to the printing solution when the process occurs in a hydrated or solvated state. Interesting

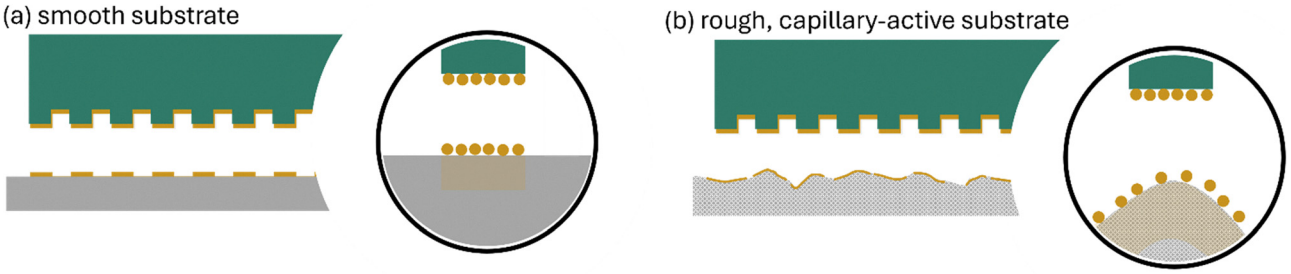

Fig. 21 Microcontact printing on different surfaces. (a) On a smooth surface, a high printing precision can be obtained. (b) On a rough, capillary-active surface, ink smearing occurs, which reduces the printing precision.

application fields in this regard would be the fabrication of patchy particulate materials,[134] which demand a very high printing precision. Moreover, patterning of bioactive surfaces,[158] such as cellular or bacterial membranes, ideally in a live state, would be a tremendously interesting application area.

A polymer matrix-assisted approach, which we refer to as PolyBrushMiC, constitutes a solution to tackle this issue. Specifically, the transfer process involves a polymer film grafted onto the stamp, which acts as an ink reservoir, allowing for a controlled transfer to the substrate. An early concept was described by Whitesides and co-workers, who used a stamp made of agarose to print protein patterns.[159] Agarose, being a natural polysaccharide, represents a hydrogel incorporating the protein ink, was used as a stamp for this purpose. In an initial study, we opted to adapt this process to other ink retention strategies. We therefore attached the commercial polymers PNIPAAm and PEG to the stamp surface, which acted as an ink reservoir to retain a rhodamine fluorescent dye used as an ink.[128] Within this film, the local viscosity of the ink is enhanced, restricting its diffusive mobility. This regulated diffusion enables a controlled transfer to the substrate, which we used to introduce confined patches to silica microspheres. This method utilized a PDMS stamp, which is chemically and mechanically more robust than agarose as a stamp material.

As an advancement of this method, we introduce the concept of PolyBrushMiC (Fig. 22a). In this approach, the ink molecule is covalently immobilized in the polymer brush matrix (approach I, Fig. 22b) and will be transferred to the substrate exclusively upon its contact with the substrate. The ink will bind thereon in a more stable fashion compared to the brush matrix.

During this process, the ink is not released and thus immobilized either in the stamp matrix or at the substrate, so that an ink diffusion and, thus, ink smearing can be entirely prevented.

The concept is in analogy to a method described by Bernard *et al.*, where the authors utilized the selective affinity of proteins at the stamp surface and the substrate for a targeted ink transfer.[162] We demonstrate this concept using a reactive silane (Fig. 22c),[131,160] specifically the transfer of APTES. As an ethanol triester of a silicic acid, APTES can be bound to a hydroxy-functional polymer brush matrix, where attaches through ester bonds. Offering an oxidic surface as a substrate, the polymer brush-bound APTES can be transferred, where it binds more stably as it binds to the brush matrix. Accordingly, we were able to prepare microscale patchy particles with highly functional patches.[134,161]

The concept of this transfer can also be applied to other chemistries. We require metastable bonds for immobilizing the ink within the polymer matrix and a stronger affinity of the ink to the substrate. The reactive transfer must occur in a concerted fashion, where the ink detachment from the polymer matrix and its attachment to the substrate occurs entirely simultaneously. The advantage of this method is that the reaction can be carried out under fully immersed conditions, making it suitable for samples prone to desiccation. An interesting example is provided by Pallab *et al.*,[158] where benzoxaborole is used as an ink (Fig. 22d). It binds to catechol moieties attached as a polymer matrix on the stamp, introduced as dopamine methacrylates, and more efficiently to glycosylated surfaces. This allowed the authors to pattern glycosylated wafers and membranes of adherent gastric cells, where the carbohydrates in the glycoprotein matrix at the membranal interface were functionalized.[158]

An alternative approach (approach II, Fig. 22b) involves immobilizing a catalyst to the stamp surface. Here, a compound that catalyses the reaction of the ink with the substrate is attached to the stamp surface. During printing, the sample is immersed in the ink solution. However, its attachment to the substrate occurs merely at the face of contact, where the catalyst meets the substrate. Mizuno *et al.* introduced this concept, using platinum particles on the surface to catalyse various Si–H coupling reactions.[163] Analogously, other immobilized catalysts can be considered. As an example, transition metal complexes or organocatalysts may be immobilized in the stamp matrix to catalyse, *e.g.* a cross-coupling or similar reaction at the substrate interface.

In order to achieve high-resolution patterning, the ink transfer – be it a *via* ink or catalyst immobilization –, the ink transfer reaction should occur as a bimolecular reaction in a concerted mechanism. Specifically, for approach I, the substrate functionalization reaction should occur simultaneously to the ink release process. In approach II, first, an ink-catalyst activated complex is formed. During the actual printing process, the activated ink should bind to the substrate simultaneously to its release from the catalyst molecule. If, however, the processes occurred as a unimolecular process, a reactive species (*i.e.* the activated ink molecule) would dissociate from the polymer matrix, where it is able to freely diffuse during the interval of its lifetime.

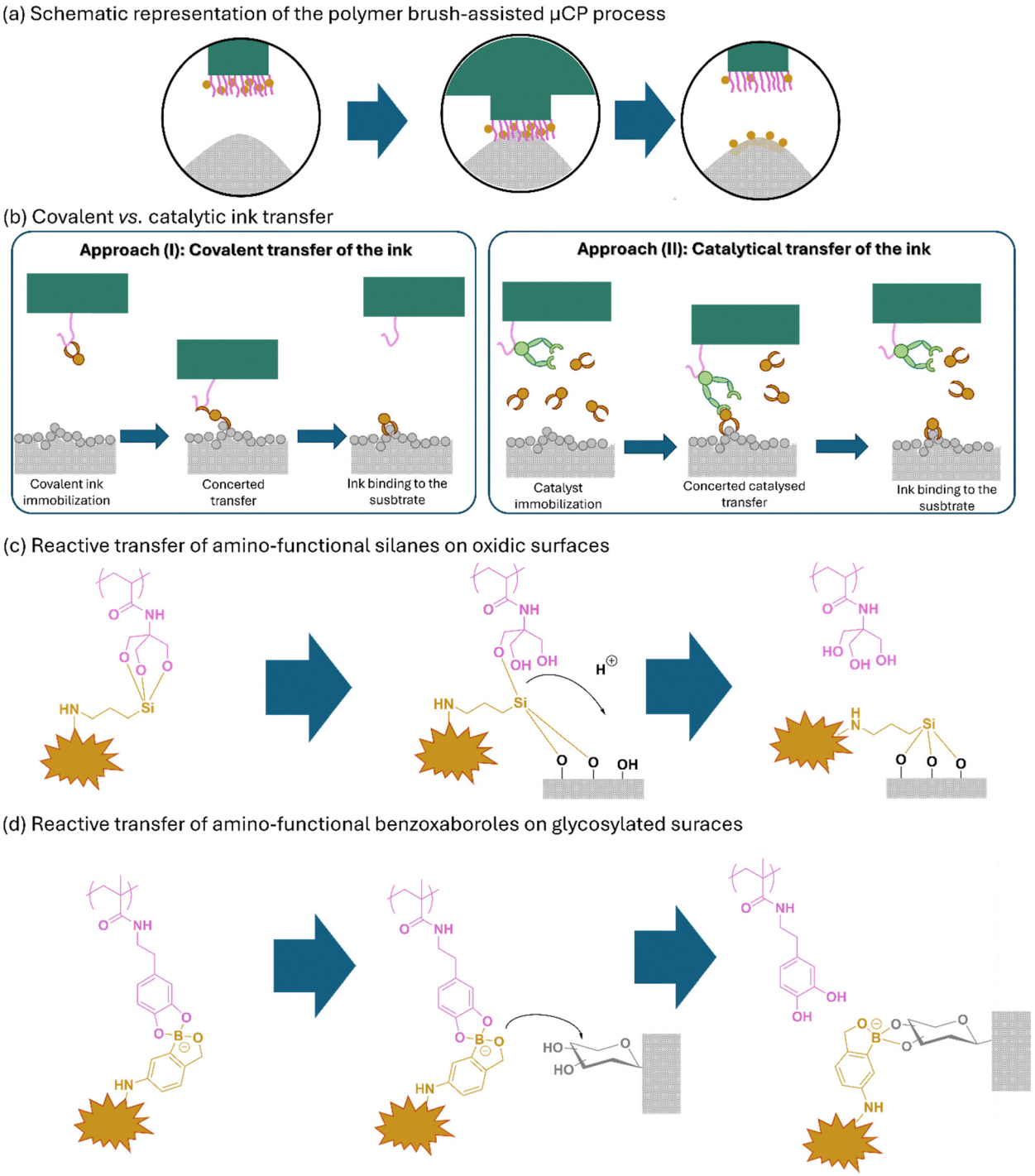

Fig. 22 Polymer brush-assisted μCP. (a) Schematic representation of the process. (b) Two ink transfer approaches are presented in this perspective. In approach (I), the ink is initially bound to the polymer brush, from where it is transferred to the substrate. (c) and (d) Examples of the PolyBrushMiC procedure. (c) Reactive transfer of silanes to oxidic surfaces.[131,134,160,161] (d) Reactive transfer of boronic acid derivatives.[158]

With the concept of PolyBrushMiC, we address the long-standing issue of ink smearing that typically hampers traditional microcontact printing (μCP). This innovative approach significantly enhances the method's versatility regarding the substrate portfolio, making it suitable for use on capillary-active, micro-rough, and even porous substrates. As a result, it opens new possibilities for surface functionalization of a wide range of materials such as zeolites, fabrics, and papers—paving the way for advanced applications in catalysis, coatings, microelectronics, and beyond. Furthermore, PolyBrushMiC extends its applicability to bio-active surfaces, enabling precise surface-modification of biological materials. This capability makes it highly valuable in fields such as tissue engineering, (stem) cell cultivation, biosensing, and regenerative medicine. Beyond, the

method allows for printing on an even smaller scale, *i.e.* nanocontact printing, thereby opening new frontiers in nanoscale patterning and device fabrication. Overall, this advancement broadens the scope of μCP, offering new opportunities for both industrial and biomedical innovations.

Conclusions

In this article, recent advancements in μCP are reviewed, encompassing the latest developments in microscale patterning and its applications in biological, microelectronic, and colloidal sciences. It is highlighted that conventional μCP methods primarily focus on patterning smooth surfaces and it is explained why rough, capillary-active substrates, and hydrogel surfaces have received less attention in literature. The challenge of ink smearing on these surfaces is addressed, which compromises printing accuracy and constitutes thus a drawback in μCP on these surfaces. As an alternative, the polymer brush-supported μCP (PolyBrushMiC) method for patterning is proposed. As a perspective, potential application areas for this technique are discussed.

Author contributions

M. R. has written and conceptualized the manuscript and has acquired funding.

Conflicts of interest

There are no conflicts to declare.

Data availability

No primary research results, software or code have been included, and no new data were generated or analysed as a part of this review.

Acknowledgements

The author thanks the German Research Foundation (Deutsche Forschungsgemeinschaft, DFG) for funding (project number: 471323994). The author acknowledges support by the University Research Focus ''Sustainable Materials Design'' of the University of Potsdam.

References

1 W. J. Hyun, E. B. Secor, M. C. Hersam, C. D. Frisbie and L. F. Francis, *Adv. Mater.*, 2015, **27**, 109–115.
2 A. Kamyshny and S. Magdassi, *Small*, 2014, **10**, 3515–3535.
3 F. Sun, H.-C. Hung, A. Sinclair, P. Zhang, T. Bai, D. D. Galvan, P. Jain, B. Li, S. Jiang and Q. Yu, *Nat. Commun.*, 2016, **7**, 13437.
4 A. Juste-Dolz, M. Avella-Oliver, R. Puchades and A. Maquieira, *Sensors*, 2018, **18**, 3163.
5 Q. Yu, P. Guan, D. Qin, G. Golden and P. M. Wallace, *Nano Lett.*, 2008, **8**, 1923–1928.
6 J. Lee, B. Yoo, H. Lee, G. D. Cha, H.-S. Lee, Y. Cho, S. Y. Kim, H. Seo, W. Lee, D. Son, M. Kang, H. M. Kim, Y. I. Park, T. Hyeon and D.-H. Kim, *Adv. Mater.*, 2017, **29**, 1603169.
7 H. Ditlbacher, J. R. Krenn, B. Lamprecht, A. Leitner and F. R. Aussenegg, *Opt. Lett.*, 2000, **25**, 563–565.
8 H. A. Atwater and A. Polman, *Nat. Mater.*, 2010, **9**, 205–213.
9 K. Vogele, J. List, G. Pardatscher, N. B. Holland, F. C. Simmel and T. Pirzer, *ACS Nano*, 2016, **10**, 11377–11384.
10 J. M. De Teresa, *Nanofabrication: Nanolithography techniques and their applications*, IOP Publishing, 2020.
11 G. Liu, M. Hirtz, H. Fuchs and Z. Zheng, *Small*, 2019, **15**, 1900564.
12 Y. Chen, *Microelectron. Eng.*, 2015, **135**, 57–72.
13 C. Vieu, F. Carcenac, A. Pépin, Y. Chen, M. Mejias, A. Lebib, L. Manin-Ferlazzo, L. Couraud and H. Launois, *Appl. Surf. Sci.*, 2000, **164**, 111–117.
14 H. X. Qian, W. Zhou, J. Miao, L. E. N. Lim and X. R. Zeng, *J. Micromech. Microeng.*, 2008, **18**, 035003.
15 W. Haufe, in *Sputtering by Particle Bombardment III: Characteristics of Sputtered Particles, Technical Applications*, ed. R. Behrisch and K. Wittmaack, Springer Berlin Heidelberg, Berlin, Heidelberg, 1991, pp. 305–338.
16 T. Kaufmann and B. J. Ravoo, *Polym. Chem.*, 2010, **1**, 371–387.
17 X. Zhou, H. Xu, J. Cheng, N. Zhao and S.-C. Chen, *Sci. Rep.*, 2015, **5**, 10402.
18 H.-W. Li, B. V. O. Muir, G. Fichet and W. T. S. Huck, *Langmuir*, 2003, **19**, 1963–1965.
19 A. Kumar and G. M. Whitesides, *Appl. Phys. Lett.*, 1993, **63**, 2002–2004.
20 Y. Xia and G. M. Whitesides, *Angew. Chem., Int. Ed.*, 1998, **37**, 550–575.
21 M. J. Jang and Y. Nam, *BioChip J.*, 2012, **6**, 107–113.
22 A. Ulman, *Chem. Rev.*, 1996, **96**, 1533–1554.
23 C. Vericat, M. E. Vela, G. Benitez, P. Carro and R. C. Salvarezza, *Chem. Soc. Rev.*, 2010, **39**, 1805–1834.
24 A. Perl, D. N. Reinhoudt and J. Huskens, *Adv. Mater.*, 2009, **21**, 2257–2268.
25 S. Alom Ruiz and C. S. Chen, *Soft Matter*, 2007, **3**, 168–177.
26 J. J. Schwartz, J. N. Hohman, E. I. Morin and P. S. Weiss, *ACS Appl. Mater. Interfaces*, 2013, **5**, 10310–10316.
27 A. Valencia Ramirez, G. Bonneux, A. Terfort, P. Losada-Pérez and F. U. Renner, *Langmuir*, 2022, **38**, 15614–15621.
28 C. A. Gunawan, M. Ge and C. Zhao, *Nat. Commun.*, 2014, **5**, 3744.
29 R. Gondosiswanto, C. A. Gunawan, D. B. Hibbert, J. B. Harper and C. Zhao, *ACS Appl. Mater. Interfaces*, 2016, **8**, 31368–31374.
30 M. Sun, J. Zhang, T. Xuanyuan, X. Liu and W. Liu, *ACS Appl. Mater. Interfaces*, 2024, **16**, 20132–20142.
31 X. Wang, M. Sperling, M. Reifarth and A. Böker, *Small*, 2020, **16**, 1906721.
32 C. Zhong, A. Kapetanovic, Y. Deng and M. Rolandi, *Adv. Mater.*, 2011, **23**, 4776–4781.

33 M. Zimmermann, D. Grigoriev, N. Puretskiy and A. Böker, *RSC Adv.*, 2018, **8**, 39241–39247.
34 M. Zimmermann, D. John, D. Grigoriev, N. Puretskiy and A. Böker, *Soft Matter*, 2018, **14**, 2301–2309.
35 D. John, M. Zimmermann and A. Böker, *Soft Matter*, 2018, **14**, 3057–3062.
36 Y. Kusaka, K. Miyashita and H. Ushijima, *J. Micromech. Microeng.*, 2014, **24**, 125019.
37 W. Cheng, X. Zeng, H. Chen, Z. Li, W. Zeng, L. Mei and Y. Zhao, *ACS Nano*, 2019, **13**, 8537–8565.
38 H.-W. Chien, W.-H. Kuo, M.-J. Wang, S.-W. Tsai and W.-B. Tsai, *Langmuir*, 2012, **28**, 5775–5782.
39 H. Wu, L. Wu, X. Zhou, B. Liu and B. Zheng, *Small*, 2018, **14**, 1802128.
40 S.-T. Han, Y. Zhou, Z.-X. Xu, L.-B. Huang, X.-B. Yang and V. A. L. Roy, *Adv. Mater.*, 2012, **24**, 3556–3561.
41 S. Gödrich, D. Brodoceanu, V. Kuznetsov, T. Kraus and G. Papastavrou, *Adv. Mater. Interfaces*, 2024, **11**, 2400202.
42 H. Li, H. Zhang, W. Luo, R. Yuan, Y. Zhao, J.-A. Huang and X. Yang, *Anal. Chim. Acta*, 2022, **1229**, 340380.
43 J. J. Gassensmith, P. M. Erne, W. F. Paxton, M. Frasconi, M. D. Donakowski and J. F. Stoddart, *Adv. Mater.*, 2013, **25**, 223–226.
44 S. Liu, W. Liu, W. Ji, J. Yu, W. Zhang, L. Zhang and W. Xie, *Sci. Rep.*, 2016, **6**, 22530.
45 H. Zhuang, B. Song, T. Staedler and X. Jiang, *Langmuir*, 2011, **27**, 11981–11989.
46 C. Wendeln and B. J. Ravoo, *Langmuir*, 2012, **28**, 5527–5538.
47 B. J. Ravoo, *J. Mater. Chem.*, 2009, **19**, 8902–8906.
48 S. Lamping, C. Buten and B. J. Ravoo, *Acc. Chem. Res.*, 2019, **52**, 1336–1346.
49 H. Li, J. Zhang, X. Zhou, G. Lu, Z. Yin, G. Li, T. Wu, F. Boey, S. S. Venkatraman and H. Zhang, *Langmuir*, 2010, **26**, 5603–5609.
50 Z. Wang, J. Xia, S. Luo, P. Zhang, Z. Xiao, T. Liu and J. Guan, *Langmuir*, 2014, **30**, 13483–13490.
51 J. Su, A. González Orive and G. Grundmeier, *Appl. Surf. Sci.*, 2023, **609**, 155355.
52 E. Färm, S. Lindroos, M. Ritala and M. Leskelä, *Chem. Mater.*, 2012, **24**, 275–278.
53 J. J. Gassensmith, P. M. Erne, W. F. Paxton, C. Valente and J. F. Stoddart, *Langmuir*, 2011, **27**, 1341–1345.
54 A. A. Shestopalov, R. L. Clark and E. J. Toone, *Nano Lett.*, 2010, **10**, 43–46.
55 A. A. Shestopalov, R. L. Clark and E. J. Toone, *Langmuir*, 2010, **26**, 1449–1451.
56 R. Castagna, A. Bertucci, E. A. Prasetyanto, M. Monticelli, D. V. Conca, M. Massetti, P. P. Sharma, F. Damin, M. Chiari, L. De Cola and R. Bertacco, *Langmuir*, 2016, **32**, 3308–3313.
57 L. Scheres, J. ter Maat, M. Giesbers and H. Zuilhof, *Small*, 2010, **6**, 642–650.
58 A. Calabretta, D. Wasserberg, G. A. Posthuma-Trumpie, V. Subramaniam, A. van Amerongen, R. Corradini, T. Tedeschi, S. Sforza, D. N. Reinhoudt, R. Marchelli, J. Huskens and P. Jonkheijm, *Langmuir*, 2011, **27**, 1536–1542.
59 Z. P. Tolstyka, W. Richardson, E. Bat, C. J. Stevens, D. P. Parra, J. K. Dozier, M. D. Distefano, B. Dunn and H. D. Maynard, *ChemBioChem*, 2013, **14**, 2464–2471.
60 H. C. Kolb, M. G. Finn and K. B. Sharpless, *Angew. Chem., Int. Ed.*, 2001, **40**, 2004–2021.
61 P. Seidel and B. J. Ravoo, *Macromol. Chem. Phys.*, 2016, **217**, 1467–1472.
62 T. Kaufmann, M. T. Gokmen, S. Rinnen, H. F. Arlinghaus, F. Du Prez and B. J. Ravoo, *J. Mater. Chem.*, 2012, **22**, 6190–6199.
63 C. Wendeln, A. Heile, H. F. Arlinghaus and B. J. Ravoo, *Langmuir*, 2010, **26**, 4933–4940.
64 T. N. Gevrek, R. N. Ozdeslik, G. S. Sahin, G. Yesilbag, S. Mutlu and A. Sanyal, *Macromol. Chem. Phys.*, 2012, **213**, 166–172.
65 J. Mehlich and B. J. Ravoo, *Org. Biomol. Chem.*, 2011, **9**, 4108–4115.
66 C. Wendeln, S. Rinnen, C. Schulz, H. F. Arlinghaus and B. J. Ravoo, *Langmuir*, 2010, **26**, 15966–15971.
67 C. Wendeln, S. Rinnen, C. Schulz, T. Kaufmann, H. F. Arlinghaus and B. J. Ravoo, *Chem. – Eur. J.*, 2012, **18**, 5880–5888.
68 N. S. Kehr, J. El-Gindi, H.-J. Galla and L. De Cola, *Microporous Mesoporous Mater.*, 2011, **144**, 9–14.
69 B. Vonhören, O. Roling, C. Buten, M. Körsgen, H. F. Arlinghaus and B. J. Ravoo, *Langmuir*, 2016, **32**, 2277–2282.
70 C. Buten, S. Lamping, M. Körsgen, H. F. Arlinghaus, C. Jamieson and B. J. Ravoo, *Langmuir*, 2018, **34**, 2132–2138.
71 C.-C. Wu, D. N. Reinhoudt, C. Otto, A. H. Velders and V. Subramaniam, *ACS Nano*, 2010, **4**, 1083–1091.
72 M. Buhl, S. Traboni, M. Körsgen, S. Lamping, H. F. Arlinghaus and B. J. Ravoo, *Chem. Commun.*, 2017, **53**, 6203–6206.
73 C. E. Neri-Cruz, F. M. E. Teixeira and J. E. Gautrot, *Chem. Commun.*, 2023, **59**, 7534–7558.
74 J. O. Zoppe, N. C. Ataman, P. Mocny, J. Wang, J. Moraes and H.-A. Klok, *Chem. Rev.*, 2017, **117**, 1105–1318.
75 B. Vonhören, M. Langer, D. Abt, C. Barner-Kowollik and B. J. Ravoo, *Langmuir*, 2015, **31**, 13625–13631.
76 T. Chen, R. Jordan and S. Zauscher, *Polymer*, 2011, **52**, 2461–2467.
77 O. Roling, A. Mardyukov, S. Lamping, B. Vonhören, S. Rinnen, H. F. Arlinghaus, A. Studer and B. J. Ravoo, *Org. Biomol. Chem.*, 2014, **12**, 7828–7835.
78 O. Roling, K. De Bruycker, B. Vonhören, L. Stricker, M. Körsgen, H. F. Arlinghaus, B. J. Ravoo and F. E. Du Prez, *Angew. Chem., Int. Ed.*, 2015, **54**, 13126–13129.
79 S. Billiet, K. De Bruycker, F. Driessen, H. Goossens, V. Van Speybroeck, J. M. Winne and F. E. Du Prez, *Nat. Chem.*, 2014, **6**, 815–821.
80 S. Lamping, L. Stricker and B. J. Ravoo, *Polym. Chem.*, 2019, **10**, 683–690.

81 S. Lamping, T. Otremba and B. J. Ravoo, *Angew. Chem., Int. Ed.*, 2018, **57**, 2474–2478.
82 M. Buhl, M. Tesch, S. Lamping, J. Moratz, A. Studer and B. J. Ravoo, *Chem. – Eur. J.*, 2017, **23**, 6042–6047.
83 T. Chen, R. Jordan and S. Zauscher, *Small*, 2011, **7**, 2148–2152.
84 F. Kettling, B. Vonhören, J. A. Krings, S. Saito and B. J. Ravoo, *Chem. Commun.*, 2015, **51**, 1027–1030.
85 P. Xiao, J. Gu, J. Chen, D. Han, J. Zhang, H. Cao, R. Xing, Y. Han, W. Wang and T. Chen, *Chem. Commun.*, 2013, **49**, 11167–11169.
86 Q. Wei, B. Yu, X. Wang and F. Zhou, *Macromol. Rapid Commun.*, 2014, **35**, 1046–1054.
87 V. T. Widyaya, E. K. Riga, C. Müller and K. Lienkamp, *Macromolecules*, 2018, **51**, 1409–1417.
88 S. Qiu, J. Ji, W. Sun, J. Pei, J. He, Y. Li, J. J. Li and G. Wang, *Smart Mater. Med.*, 2021, **2**, 65–73.
89 M. Buhl, B. Vonhören and B. J. Ravoo, *Bioconjugate Chem.*, 2015, **26**, 1017–1020.
90 M. Wiens, T. Link, T. A. Elkhooly, S. Isbert and W. E. G. Müller, *Chem. Commun.*, 2012, **48**, 11331–11333.
91 M. Ganesh, J. Nachman, Z. Mao, A. Lyons, M. Rafailovich and R. Gross, *Biomacromolecules*, 2013, **14**, 2470–2476.
92 F. M. Watt and W. T. S. Huck, *Nat. Rev. Mol. Cell Biol.*, 2013, **14**, 467–473.
93 C. J. Bettinger, R. Langer and J. T. Borenstein, *Angew. Chem., Int. Ed.*, 2009, **48**, 5406–5415.
94 C. Leclech and C. Villard, *Front. Bioeng. Biotechnol.*, 2020, **8**, 551505.
95 S. Hu, T.-H. Chen, Y. Zhao, Z. Wang and R. H. W. Lam, *Langmuir*, 2018, **34**, 1750–1759.
96 A. B. C. Buskermolen, T. Ristori, D. Mostert, M. C. van Turnhout, S. S. Shishvan, S. Loerakker, N. A. Kurniawan, V. S. Deshpande and C. V. C. Bouten, *Cell Rep. Phys. Sci.*, 2020, **1**, 100055.
97 K. Steiner and C. Humpel, *Biomolecules*, 2024, **14**, 3.
98 K. Steiner and C. Humpel, *Front. Biosci., Landmark Ed.*, 2024, **29**, 232.
99 C. D. Eichinger, T. W. Hsiao and V. Hlady, *Langmuir*, 2012, **28**, 2238–2243.
100 K. Steiner and C. Humpel, *J. Neurosci. Methods*, 2023, **399**, 109979.
101 R. Fricke, P. D. Zentis, L. T. Rajappa, B. Hofmann, M. Banzet, A. Offenhäusser and S. H. Meffert, *Biomaterials*, 2011, **32**, 2070–2076.
102 L. Wong, J. D. Pegan, B. Gabela-Zuniga, M. Khine and K. E. McCloskey, *Biofabrication*, 2017, **9**, 021001.
103 E. Blinka, K. Loeffler, Y. Hu, A. Gopal, K. Hoshino, K. Lin, X. Liu, M. Ferrari and J. X. J. Zhang, *Nanotechnology*, 2010, **21**, 415302.
104 E. Kosobrodova, W. J. Gan, A. Kondyurin, P. Thorn and M. M. M. Bilek, *ACS Appl. Mater. Interfaces*, 2018, **10**, 227–237.
105 M. J. Jang and Y. Nam, *Macromol. Biosci.*, 2015, **15**, 613–621.
106 J. Borowiec, J. Hampl, S. Singh, S. Haefner, K. Friedel, P. Mai, D. Brauer, F. Ruther, L. Liverani, A. R. Boccaccini and A. Schober, *ACS Appl. Mater. Interfaces*, 2018, **10**, 22857–22865.
107 S. Sathish, S. G. Ricoult, K. Toda-Peters and A. Q. Shen, *Analyst*, 2017, **142**, 1772–1781.
108 L. E. Corum, C. D. Eichinger, T. W. Hsiao and V. Hlady, *Langmuir*, 2011, **27**, 8316–8322.
109 S. Engin, V. Trouillet, C. M. Franz, A. Welle, M. Bruns and D. Wedlich, *Langmuir*, 2010, **26**, 6097–6101.
110 S. Lowe, N. M. O'Brien-Simpson and L. A. Connal, *Polym. Chem.*, 2015, **6**, 198–212.
111 Z. Wang, P. Zhang, B. Kirkland, Y. Liu and J. Guan, *Soft Matter*, 2012, **8**, 7630–7637.
112 H.-W. Chien and W.-B. Tsai, *Acta Biomater.*, 2012, **8**, 3678–3686.
113 N. Tanaka, H. Ota, K. Fukumori, J. Miyake, M. Yamato and T. Okano, *Biomaterials*, 2014, **35**, 9802–9810.
114 Y. B. Lee, S. Kim, E. M. Kim, H. Byun, H. Chang, J. Park, Y. S. Choi and H. Shin, *Acta Biomater.*, 2017, **61**, 75–87.
115 A. G. Castaño, V. Hortigüela, A. Lagunas, C. Cortina, N. Montserrat, J. Samitier and E. Martínez, *RSC Adv.*, 2014, **4**, 29120–29123.
116 S. G. Ricoult, A. Sanati Nezhad, M. Knapp-Mohammady, T. E. Kennedy and D. Juncker, *Langmuir*, 2014, **30**, 12002–12010.
117 Z. Wang, J. Xia, Y. Yan, A.-C. Tsai, Y. Li, T. Ma and J. Guan, *Acta Biomater.*, 2015, **11**, 80–87.
118 J.-P. Frimat, M. Bronkhorst, B. de Wagenaar, J. G. Bomer, F. van der Heijden, A. van den Berg and L. I. Segerink, *Lab Chip*, 2014, **14**, 2635–2641.
119 H. Yu, S. Xiong, C. Y. Tay, W. S. Leong and L. P. Tan, *Acta Biomater.*, 2012, **8**, 1267–1272.
120 S. Ravaine and E. Duguet, *Curr. Opin. Colloid Interface Sci.*, 2017, **30**, 45–53.
121 H. Su, C.-A. Hurd Price, L. Jing, Q. Tian, J. Liu and K. Qian, *Mater. Today Bio*, 2019, **4**, 100033.
122 Y. Huang, C. Wu, J. Chen and J. Tang, *Angew. Chem., Int. Ed.*, 2024, **63**, e202313885.
123 W. Li, H. Palis, R. Mérindol, J. Majimel, S. Ravaine and E. Duguet, *Chem. Soc. Rev.*, 2020, **49**, 1955–1976.
124 F. Naderi Mehr, D. Grigoriev, R. Heaton, J. Baptiste, A. J. Stace, N. Puretskiy, E. Besley and A. Böker, *Small*, 2020, **16**, 2000442.
125 F. N. Mehr, D. Grigoriev, N. Puretskiy and A. Böker, *Soft Matter*, 2019, **15**, 2430–2438.
126 P. Zhang and J. Guan, *Small*, 2011, **7**, 2998–3004.
127 T. Kaufmann, M. T. Gokmen, C. Wendeln, M. Schneiders, S. Rinnen, H. F. Arlinghaus, S. A. F. Bon, F. E. Du Prez and B. J. Ravoo, *Adv. Mater.*, 2011, **23**, 79–83.
128 M. Sperling, M. Reifarth, R. Grobe and A. Böker, *Chem. Commun.*, 2019, **55**, 10104–10107.
129 T. Kaufmann, C. Wendeln, M. T. Gokmen, S. Rinnen, M. M. Becker, H. F. Arlinghaus, F. Du Prez and B. J. Ravoo, *Chem. Commun.*, 2013, **49**, 63–65.
130 S. Sagebiel, L. Stricker, S. Engel and B. J. Ravoo, *Chem. Commun.*, 2017, **53**, 9296–9299.
131 P. Akarsu, R. Grobe, J. Nowaczyk, M. Hartlieb, S. Reinicke, A. Böker, M. Sperling and M. Reifarth, *ACS Appl. Polym. Mater.*, 2021, **3**, 2420–2431.

132 M. Hartlieb, *Macromol. Rapid Commun.*, 2022, **43**, 2100514.
133 A.-C. Lehnen, J. A. M. Kurki and M. Hartlieb, *Polym. Chem.*, 2022, **13**, 1537–1546.
134 M. Reifarth, M. Sperling, R. Grobe, P. Akarsu, F. Schmitt, M. Schmette, S. Tank, K. M. Arndt, S. Chiantia, M. Hartlieb and A. Böker, *Adv. Funct. Mater.*, 2025, 2423495.
135 J. Mehlich, Y. Miyata, H. Shinohara and B. J. Ravoo, *Small*, 2012, **8**, 2258–2263.
136 X. Du, R. T. Frederick, Y. Li, Z. Zhou, W. F. Stickle and G. S. Herman, *J. Vac. Sci. Technol., B*, 2015, **33**, 052208.
137 O. Kina, M. Koutake, K. Matsuoka and K. Yase, *Jpn. J. Appl. Phys.*, 2010, **49**, 01AB07.
138 E. P. Yalcintas, K. B. Ozutemiz, T. Cetinkaya, L. Dalloro, C. Majidi and O. B. Ozdoganlar, *Adv. Funct. Mater.*, 2019, **29**, 1906551.
139 B. A. Gozen, A. Tabatabai, O. B. Ozdoganlar and C. Majidi, *Adv. Mater.*, 2014, **26**, 5211–5216.
140 F. E. Hizir, M. R. Hale and D. E. Hardt, *J. Micromech. Microeng.*, 2020, **30**, 115008.
141 Z. Xin, Y. Liu, X. Li, S. Liu, Y. Fang, Y. Deng, C. Bao and L. Li, *Mater. Res. Express*, 2017, **4**, 015021.
142 G. Mondin, B. Schumm, J. Fritsch, J. Grothe and S. Kaskel, *Microelectron. Eng.*, 2013, **104**, 100–104.
143 S. Gout, J. Coulm, D. Léonard and F. Bessueille, *Appl. Surf. Sci.*, 2014, **307**, 716–723.
144 S.-S. Yoon and D.-Y. Khang, *ACS Appl. Mater. Interfaces*, 2016, **8**, 23236–23243.
145 M. S. Miller, H. L. Filiatrault, G. J. E. Davidson, M. Luo and T. B. Carmichael, *J. Am. Chem. Soc.*, 2010, **132** 765–772.
146 F. M. Wisser, B. Schumm, A. Meier, T. Engel, J. Grothe, G. Kickelbick and S. Kaskel, *J. Mater. Chem. C*, 2013, **1**, 2477–2484.
147 A. Tabatabai, A. Fassler, C. Usiak and C. Majidi, *Langmuir*, 2013, **29**, 6194–6200.
148 P. Xiao, J. Gu, J. Chen, J. Zhang, R. Xing, Y. Han, J. Fu, W. Wang and T. Chen, *Chem. Commun.*, 2014, **50**, 7103–7106.
149 S.-W. Choi, W.-S. Kang, J.-H. Lee, C. K. Najeeb, H.-S. Chun and J.-H. Kim, *Langmuir*, 2010, **26**, 15680–15685.
150 A. Béduer, F. Seichepine, E. Flahaut and C. Vieu, *Microelectron. Eng.*, 2012, **97**, 301–305.
151 H. Ogihara, H. Kibayashi and T. Saji, *ACS Appl. Mater. Interfaces*, 2012, **4**, 4891–4897.
152 K. Fuchsberger, A. L. Goff, L. Gambazzi, F. M. Toma, A. Goldoni, M. Giugliano, M. Stelzle and M. Prato, *Small*, 2011, **7**, 524–530.
153 A. Garcia-Cruz, N. Zine, M. Sigaud, M. Lee, P. Marote, P. Lanteri, J. Bausells and A. Errachid, *Microelectron. Eng.*, 2014, **121**, 167–174.
154 S. G. Croll, *Prog. Org. Coat.*, 2020, **148**, 105847.
155 C. M. A. Parlett, K. Wilson and A. F. Lee, *Chem. Soc. Rev.*, 2013, **42**, 3876–3893.
156 X. Xu, W. Wang, Y. Liu, J. Bäckemo, M. Heuchel, W. Wang, Y. Nie, I. Iqbal, K. Kratz, A. Lendlein and N. Ma, *Nat. Mater.*, 2024, **23**, 1748–1758.
157 J. Lou and D. J. Mooney, *Nat. Rev. Chem.*, 2022, **6**, 726–744.
158 N. Pallab, E. Sperlich, M. Schenderlein, A. Krüger-Genge, J. Li, L. Zeininger, Z. Tošner, M. Uchman and M. Reifarth, *Angew. Chem., Int. Ed.*, 2025, e202501759.
159 M. Mayer, J. Yang, I. Gitlin, D. H. Gracias and G. M. Whitesides, *Proteomics*, 2004, **4**, 2366–2376.
160 N. Pallab, S. Reinicke, J. Gurke, R. Rihm, S. Kogikoski, M. Hartlieb and M. Reifarth, *Polym. Chem.*, 2024, **15**, 853–867.
161 P. Akarsu, S. Reinicke, A.-C. Lehnen, M. Bekir, A. Böker, M. Hartlieb and M. Reifarth, *Small*, 2023, **19**, 2301761.
162 A. Bernard, D. Fitzli, P. Sonderegger, E. Delamarche, B. Michel, H. R. Bosshard and H. Biebuyck, *Nat. Biotechnol.*, 2001, **19**, 866–869.
163 H. Mizuno and J. M. Buriak, *ACS Appl. Mater. Interfaces*, 2009, **1**, 2711–2720.

